



Review

FRET analysis of domain formation and properties in complex membrane systems

Luís M.S. Loura^{a,b,*}, Rodrigo F.M. de Almeida^c, Liana C. Silva^d, Manuel Prieto^d^a Faculdade de Farmácia, Universidade de Coimbra, R. do Norte, 3000-295 Coimbra, Portugal^b Centro de Química de Évora, R. Romão Ramalho, 59, 7000-671 Évora, Portugal^c Centro de Química e Bioquímica, Faculdade de Ciências da Universidade de Lisboa, R. Ernesto de Vasconcelos, 1749-016 Lisboa, Portugal^d Centro de Química-Física Molecular and Institute of Nanosciences and Nanotechnologies, Complexo I, Instituto Superior Técnico, Av. Rovisco Pais, 1049-001 Lisboa, Portugal

ARTICLE INFO

Article history:

Received 30 August 2008

Received in revised form 16 October 2008

Accepted 16 October 2008

Available online 30 October 2008

Keywords:

Fluorescence

Lipid bilayer

Lipid raft

Membrane phase separation

Phase diagram

ABSTRACT

The application of Förster Resonance Energy Transfer (FRET) to the detection and characterization of phase separation in lipid bilayers (both in model systems and in cell membranes) is reviewed. Models describing the rate and efficiency of FRET for both uniform probe distribution and phase separation, and recently reported methods for detection of membrane heterogeneity and determination of phase boundaries, probe partition coefficients and domain size, are presented and critically discussed. Selected recent applications of FRET to one-phase lipid systems, gel/fluid phase separation, liquid ordered/liquid disordered phase separation (lipid rafts), complex systems containing ceramide and cell membranes are presented to illustrate the wealth of information that can be inferred from carefully designed FRET studies of membrane domains.

© 2008 Elsevier B.V. All rights reserved.

Contents

1. Introduction – on phases, domains and sizes	209
2. Phase diagrams of lipid mixtures	210
3. Basic FRET formalisms in membranes	211
4. Applications	213
4.1. One-phase lipid systems	214
4.2. Binary phospholipid mixtures with gel/fluid phase separation	215
4.3. ld/lo phase separation	216
4.4. Gel/ld/lo phase separation	219
4.5. FRET studies of nano and microdomains of lipids and proteins in cell membranes.	221
5. Concluding remarks	222
Acknowledgements	222
References	222

1. Introduction – on phases, domains and sizes

After the first important paradigm of membrane structure, the fluid mosaic model [1], it is by now well established in the field of membrane biophysics that non-homogeneous lateral distribution of lipid components exists both in natural and model membranes. This non-homogeneity is a thermodynamic imperative, since in general lipids do not make an ideal solution, and therefore this is only due to

lipid–lipid interaction, although the presence of proteins can induce perturbations in this process. Therefore, under a situation of thermodynamic equilibrium, phase diagrams can be derived, and examples dating back to 1990 (at the time only a few binary mixtures were studied, and ternary lipid systems were not yet explored), were compiled by Marsh [2].

The relevant phases upon mixing lipids with different transition temperatures are gel and fluid, and for phospholipid/cholesterol mixtures, the concept of liquid ordered (lo) and liquid disordered (ld) phases was introduced by Ipsen et al. [3].

Later, the concept of lipid rafts was proposed [4]. These were at first operationally defined as insoluble membrane fractions upon

* Corresponding author. Faculdade de Farmácia, Universidade de Coimbra, R. do Norte, 3000-295 Coimbra, Portugal. Tel.: +351 239859950; fax: +351 239827126.

E-mail address: lloura@ff.uc.pt (L.M.S. Loura).

detergent extraction (the so-called “detergent resistant membranes”, DRM), and their composition revealed that they were rich in cholesterol, sphingomyelin and unsaturated lipids. These membrane patches, which were intensively studied both in membrane biophysics and cell biology, were described as liquid-ordered on the framework of the above mentioned type of phases postulated in the presence of cholesterol. Although membrane heterogeneity was not a novelty in itself, the very pictorial raft concept bridged the fields of membrane biophysics and cell biology, and the communication between these two communities was instrumental to develop a very active research on membranes in both natural and model systems.

Several interconnected concepts can be misleading, among them phases and membrane domains, and also the problem of their sizes. Phases and phase diagrams only apply to systems under thermodynamic equilibrium, and it should be stressed that this situation can be a very slow process. In a situation of very strong mismatch of two lipid components, i.e. even when the driving force is very high, the time needed to attain equilibrium upon a system perturbation can be on the timescale of hours for gel/fluid phase separation [5–7]. However, even considering that a cell membrane is not under equilibrium, phase diagrams are instrumental in the rationalization of the processes that can occur in a natural membrane. Also according to thermodynamic considerations, phase separation would proceed until completion in order to decrease line tension, so this would imply that the observed domains, whatever the methodology used, should be very large. This is observed for gel/fluid phase separation where the phase boundary is very steep, and defects are present. However for liquid-ordered/liquid disordered phase coexistence the domains can be small (submicron, “nanodomains”), as will be discussed later in detail in this review, and cholesterol or specified lipid configurations have been invoked as able to reduce line tension, therefore preventing their growth [8]. It should be stressed that increasing the number of domains also leads to an entropic compensation.

The existing discussion in the literature about domain sizes was prompted by the distinct information obtained according to the different type of experimental approach used to detect and study them. While in natural membranes there is clear evidence that domains are in general small (10–100 nm, nanodomains) (see e.g., [9–11]), in model systems different answers were obtained depending on the methodology used. Under a confocal microscope, large (micron size) domains can be observed in suitable systems, namely ternary systems with ld/lo phase coexistence, but up to now no domains were observed for binary systems with cholesterol [12]. This is in general attributed to the very small size of these lo domains, below the lateral resolution of the microscope (~300 nm), and it prompts a global discussion about the type of phase diagrams (and so the phases and domains sizes) that are described in the literature. There is a clear disagreement when comparing the ones coming from microscopy data, with the ones obtained from spectroscopic approaches such as fluorescence and ESR as described by e.g., [13]. From fluorescence spectroscopy, as described later in this review and using Förster Resonance Energy Transfer (FRET) with adequate modeling, clear evidence for nanoscopic domains is obtained and the same happens e.g., from residence time data in the submicrosecond regime in ESR spectroscopy [14]. Therefore, more detail is obtained from spectroscopic approaches which do not miss the existence of small domains. Along this way a recent work [15] favors the utilization of spectroscopic diagrams. Microscopy is however invaluable in the way that it allows direct visualization of lipid domains, and we can foresee in the future fast development in this area, such as STED (stimulated emission depletion microscopy [16]), which allows a closer to molecular resolution (~30 nm) as compared to standard confocal (~300 nm). Also recently, in a powerful conjunction with AFM (e.g., [17]), this technique proves highly useful in the study of membrane domains.

Another subject under discussion is if the nanodomains (assuming they are not transient density fluctuations), should be considered as phases, as otherwise the phase diagrams based on their detection, as well as the respective tie-lines, would have no meaning. Apart from the problem that phase separation will not go to completion as discussed before (but the same happens for the larger micron size domains detected by microscopy), there is no critical restriction on size that would prevent the phase concept of being applied to them. In addition domains larger than ~25 nm are formed by >1000 molecules, i.e., they are large enough for their rationalization as a phase in the framework of statistical thermodynamics. Another relevant aspect is that spectroscopic methodologies allow the derivation of phase diagrams that are thermodynamically consistent.

It should be mentioned that biological membranes and their model systems are a very lively research area, and also the concept of cholesterol-induced lo/ld phase separation above mentioned [3] has been questioned in recent literature using different approaches, such as e.g., X-ray diffraction [18] and NMR data [19]. However, in this review the discussion about phases and cholesterol will be carried out in the framework of that type of phase separation, which was revealed to be instrumental in the rationalization of membrane biophysics.

2. Phase diagrams of lipid mixtures

Binary and tertiary phase diagrams have long been used as invaluable tools in fields such as mineralogy, metallurgy and material science. The most commonly used phase diagrams of binary lipid bilayers are temperature (T)/composition (x) diagrams, in which pressure is constant (most often 1 atm) and the lines (phase boundaries) separate (x, T) regions corresponding to different stable phases. Crossing these equilibrium lines implies the occurrence of one or more phase transitions. For a given (x, T) point inside a two-phase region, the horizontal (constant T) straight line connecting the point under consideration to the phase boundaries located at either side of it is termed a tie-line. From the abscissas of the extremes of the tie-line (their points of intersection with the phase boundaries), the compositions of the phases in equilibrium are obtained. On the other hand, the relative distances along the tie-line between the two-phase point and the phase boundaries give the proportion of each phase in the mixture (lever rule, see Fig. 1 for graphical example).

There is an additional degree of freedom in ternary mixtures, and therefore, in order to be represented in a two-dimensional diagram,

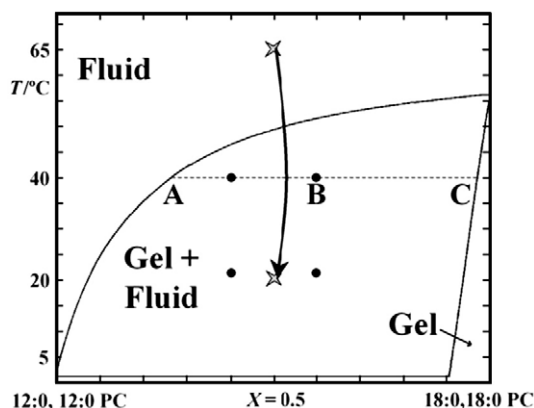


Fig. 1. Phase diagram for 12:0,12:0 PC/18:0,18:0 vesicles (adapted from [57]), illustrating i) the tie-line for $T=40^{\circ}\text{C}$, [AC]. The composition of the phases in equilibrium for any point along this line is given by the abscissas of points A and C for the fluid and the gel, respectively. Using the lever rule, the gel and fluid fractions in the mixture with 60 mol% 18:0,18:0 PC globally (point B) are given by $\overline{AB}/\overline{AC}$ and $\overline{BC}/\overline{AC}$, respectively; ii) the points inside the phase gel/fluid coexistence range (filled circles) studied by FRET in [31]; iii) the initial and final points (grey stars) after the thermal quench (represented schematically by the curved arrow) in the phase separation kinetics study mentioned in the text [6].

the phase boundaries of ternary diagrams (which take the shape of a triangle, with one component at each corner and a binary mixture at each side) are often represented for fixed pressure and temperature. In this case, the tie-lines are no longer horizontal and must be obtained experimentally, which can be a very complex and time-consuming task. However, knowledge of the tie-lines is still of paramount importance, because, as in binary diagrams, the composition of each coexisting phase is invariant along the tie-line and the lever rule is valid. Meaningful studies of partition between two coexisting lipid phases and FRET as a probe of lipid domain size require working along a tie-line, as will be illustrated and discussed in detail below.

Although phase diagrams are essential starting points for the study of lipid mixtures, they do not contain all relevant information concerning a particular lipid system. In particular, as mentioned in the preceding section, they are not informative about domain size and shape. Unlike bulk phase separation, domain formation in lipid systems is not necessarily expected to proceed to completion, given that the line tension separating different phases is expected to be low and domains can be stabilized in several distinct ways [20,21]. Estimation of domain sizes in different lipid systems using FRET techniques will be addressed below.

3. Basic FRET formalisms in membranes

The formalisms of FRET in a plane and to a plane of acceptors parallel to that of donors, and how they can be combined to obtain the FRET kinetic law for a particular system have been reviewed [22,23]. Briefly, quenching of the donor excited state (whose lifetime in absence of acceptor is τ_0) by FRET to an acceptor located at a relative distance R follows first order kinetics, the rate constant being given by [24]

$$k_T = \frac{1}{\tau_0} \left(\frac{R_0}{R} \right)^6 \quad (1)$$

where R_0 , the Förster critical distance, is calculated (in Å units) from

$$R_0 = 0.2108 \left[\kappa^2 \Phi_0 n^{-4} \int_0^\infty \lambda^4 I(\lambda) \varepsilon(\lambda) d\lambda \right]^{1/6} \quad (2)$$

where in turn κ^2 is the orientation factor (see [25] for a detailed discussion), Φ_0 is the donor quantum yield in the absence of acceptor, n is the refractive index, λ is the wavelength (in nm units), $I(\lambda)$ is the normalized donor emission spectrum, and $\varepsilon(\lambda)$ is the acceptor molar absorption spectrum.

In the remainder of this section it is assumed that the donor and acceptor fluorophores are non-identical (hetero-FRET). The considerably more complex, much less frequently used case of identical donor and acceptor fluorophores (homo-FRET) does not lead to an overall fluorescence quenching, and is only detectable from polarized fluorescence measurements [25]. Almost all the results described in Section 4 came from hetero-FRET measurements, and those retrieved from homo-FRET are identified as such in the text.

For non-identical donor and acceptor, from the reduction in donor quantum yield or lifetime when in presence of acceptor, the extent of FRET can be quantified. It is often operationally reported by the FRET efficiency, E , which is defined by

$$E = 1 - \frac{\int_0^\infty i_{DA}(t) dt}{\int_0^\infty i_D(t) dt} \quad (3)$$

where $i_D(t)$ and $i_{DA}(t)$ are the donor decays in absence and presence of acceptor, respectively. For exponentially decaying donor excited state, Eq. 3 reduces to

$$E = 1 - \tau / \tau_0 \quad (4)$$

An expression identical to Eq. 4 can be written for the fluorescence quantum yield, replacing τ_0 and τ with Φ_0 and Φ ,

respectively (the latter being the fluorescence quantum yield in presence of acceptor).

From either steady-state (fluorescence intensity) or time-resolved data (fluorescence lifetime), R is easily computed:

$$R = \left(\frac{1-E}{E} \right)^{1/6} R_0 \quad (5)$$

The latter equation is the basis of the use of FRET as a “spectroscopic ruler” [26]. It should be stressed that its validity is restricted to the situation where all donor/acceptor pairs have the same separation distance, R . Using Eq. 5, it is readily shown that virtually all change in E occurs in a relatively narrow distance range, as this parameter increases from 1 to 99% when R varies from $2.15R_0$ to $0.46R_0$. For most of the useful donor/acceptor pairs R_0 falls between 2 and 6 nm. This justifies that, for constant donor/acceptor separation, FRET probes most usefully the 1–10 nm length range. This condition is seldom met in membrane studies, for which donors and acceptors are scattered in the bilayer, resulting in multiple donor–acceptor distances. In this case, the efficiency of FRET may still be quantified from Eq. 3, but the use of Eq. 5 does not lead to a physically precise and meaningful donor–acceptor distance, and should be avoided in this context.

In practice, lipid vesicles provide an infinite planar or quasi-planar geometry for FRET purposes (because their curvature radii are much larger than R_0). This allows the derivation of analytical expressions for the donor decay in presence of acceptor. When donors and acceptors are in the same plane (*cis* transfer), and additionally there is no homo-FRET between donors, the fraction of excited acceptors is negligible, and no translational diffusion is taking place during the excited donor lifetime, the result is [27,28]

$$i_{DA,cis}(t) = \exp\left(-\frac{t}{\tau_0}\right) \exp\left\{-\pi R_0^2 n \gamma \left[\frac{2}{3}, \left(\frac{R_0}{R_e}\right)^6 \left(\frac{t}{\tau_0}\right)\right] \left(\frac{t}{\tau_0}\right)^{1/3}\right\} \cdot \exp\left\{\pi R_e^2 n \left(1 - \exp\left[-\left(\frac{R_0}{R_e}\right)^6 \left(\frac{t}{\tau_0}\right)\right]\right)\right\} \quad (6)$$

where n is the number of acceptors per unit area, γ is the incomplete gamma function, and R_e is the distance of closest approach between donor and acceptor molecules. In case that $R_e \ll R_0$ (in practice, if $R_e < R_0/4$), Eq. 6 reduces to

$$i_{DA,cis}(t) = \exp(-t/\tau_0) \exp(-C(t/\tau_0)^{1/3}) \quad (7)$$

where

$$C = \Gamma(2/3) n \pi R_0^2 \quad (8)$$

In the latter equation, Γ is now the complete gamma function.

Frequently, donors and acceptors are located in parallel planes (separated by an interplane distance l), as a result of different transverse membrane locations. In this case, the result for the donor decay law is [29]:

$$i_{DA,trans}(t) = \exp(-t/\tau_0) \exp(-kCl^2 F(l, t, R_e)) \quad (9)$$

where

$$F(l, t, R_e) = \int_0^{\frac{l}{\sqrt{l^2 + R_e^2}}} \frac{1 - \exp\left(-t/\tau_0\right) \left(R_0/l\right)^6 \alpha^6}{\alpha^3} d\alpha \quad (10)$$

and $k=2/R_0^2$. If $R_e \ll R_0$, the upper limit in the integral in Eq. 10 becomes 1. If each donor can transfer energy to two or more distinct planes of acceptors, then $i_{DA}(t)$ is obtained by multiplying the intrinsic donor decay by the survival probability terms (second exponential terms in the right hand side of Eqs. 6, 7 or 9) pertinent to each acceptor plane. In all cases, the experimental FRET efficiency is computed and

compared to the theoretical expectation (obtained by inserting the theoretical decay law in Eq. 3; analytical expressions are also given in [28] in the simpler cases of a single acceptor plane), or (preferably) the experimental decay is analyzed using fitting algorithms which implement the complex theoretical decay kinetics for direct recovery of the model parameters.

Frequently, the decay of the donor fluorophore in membranes is nonexponential, and can only be satisfactorily described using a sum of exponentials. In this situation, the first exponential term in the right hand side of Eqs. 6, 7 and 9 should be replaced by this function, whereas τ_0 should be replaced by the average lifetime (also called intensity-weighted averaged lifetime) in the second term. For calculation of the FRET efficiency using Eq. 4, lifetime-weighted quantum yields (also called amplitude-weighted averaged lifetimes) should be used [30].

Non-uniform component distribution and phase separation are common occurrences in lipid mixtures. Donor and acceptor fluorophores in such a system will naturally have non-uniform distributions, reflecting their partition between the coexisting phase domains. In the simplest case, there are only two phases or types of domains present. If these are sufficiently large to be infinite in the FRET scale (larger than $\sim 5\text{--}10 R_0$), complications resulting from FRET involving molecules in different domains, or boundary effects, are negligible, and the donor decay law is simply a linear combination of the decay laws in each phase, weighed by the relative amount of donor (A_i) in each phase [31]:

$$i_{\text{DA, phase separation}}(t) = A_1 i_{\text{DA, phase 1}}(t) + A_2 i_{\text{DA, phase 2}}(t) \quad (11)$$

$i_{\text{DA}}(t)$ within each phase is calculated as outlined above. Usually the donor lifetimes are different in the two phases, as are the acceptor surface concentrations, and possibly also the distances between donor and acceptor planes. This implies that, for more accurate parameter recovery, decay of donor in presence of acceptor should be globally analyzed together with that in the absence of acceptor,

$$i_{\text{D}}(t) = A_1 \exp(-t/\tau_1) + A_2 \exp(-t/\tau_2) \quad (12)$$

where τ_1 and τ_2 are the donor lifetimes in each phase (for nonexponentially decaying donors, the modifications described above should be observed). The recovered parameters are usually τ_1 , τ_2 , A_2/A_1 (from which the donor partition coefficient K_{pD} is obtained), and the acceptor concentrations in the two phases, C_1 and C_2 (from which the acceptor partition coefficient K_{pA} is obtained) [22]. A particular case of this formalism is the so-called “isolated donors” limit, which corresponds to $C_2=0$ [32].

The utility of FRET in the study of membrane nanodomains stems from the natural distance sensitivity of the phenomenon, coupled with the compartmentalization resulting from domain formation. In this context, it is convenient to choose probes with a strong marked preference for one of the domain types. Typically donors will prefer the domains and acceptors the continuous phase, or vice-versa. In this scenario, domain formation prompts increased donor–acceptor separation and therefore decreased FRET efficiency. Because probes within a domain are scattered inside it, with high probability of location near the domain boundaries, the range of domain sizes probed by FRET is shifted to higher values relative to the 0.5–2 nm range for the constant donor/acceptor separation distance case discussed above. Analysis of synthetic decays or efficiencies produced by numerical simulations with analytical models revealed that whereas domains of size $\sim 10R_0$ (50 nm for a typical $R_0=5$ nm value) are already difficult to distinguish from infinite phases, FRET is particularly sensitive to small domains, in the $2R_0\text{--}4R_0$ ($\sim 10\text{--}20$ nm) range [33,34]. In the limit of domain size $<R_0$, the probe distribution becomes increasingly closer to uniform, and the donor decay differs negligibly from that in the absence of domain formation. This type of heterogeneity (domains with clearly <100 molecules) can eventually

be detected from parameters that only depend on the immediate vicinity of the probes, such as fluorescence anisotropy, lifetime or intensity, if these vary considerably from the domain environment to the bulk phase.

Most recent FRET studies in the context of lipid domains fall in one of two categories: either the phase diagram of the system is unknown, and FRET is used to probe eventual heterogeneity, or the phase diagram has been obtained from independent measurements, and FRET is used to probe domain size inside the previously defined coexistence range. In the latter situation, and similarly to the determination of the partition coefficient between two coexisting lipid phases, the application of FRET requires that all the studied compositions are located along a tie-line. Otherwise, the phases in equilibrium have non-constant composition, rendering the whole study at best difficult to rationalize.

Buboltz [35] derived a procedure (“Steady-State Probe-Partitioning FRET” or SP-FRET), based on measurement of acceptor sensitized emission of different FRET pairs in the same phase separated system, that, for given tie-lines and phase boundaries, allows the determination of the probes’ interphasic partition coefficients as the sole fitting parameters. The intrinsic sensitized emission of a given FRET pair in a particular lipid phase is modelled as a function of the acceptor mole fraction that reproduces the asymptotic behaviours for low and high acceptor concentrations, and reduces to a particularly simple form in the former limit [36]. The requirement of previous knowledge of the phase boundaries and tie-lines may be alleviated by estimating them from the compositions where the gradient of acceptor sensitized emission is maximal, as shown by the author using FRET with pairs made up of dehydroergosterol (DHE) and carbocyanine dyes in the 12:0,12:0 phosphatidylcholine (PC)/16:0,16:0 PC lipid mixture (in this notation, $m:n$ denotes an acyl chain with m carbon atoms and n double bonds, the first chain being the $sn-1$ one) [35]. The application of SP-FRET requires the infinite phase separation condition, which can be achieved by choosing a pair with small R_0 value. Therefore, this method is a tool to probe phase boundaries, but not domain sizes. Application of this technique to a ternary raft model system is described in Subsection 4.3.

Since Eq. 11 is strictly valid only for infinite phase separation, its application to nano-scale domains leads to the recovery of an acceptor partition coefficient (“FRET” K_{pA}) unequal to the true coefficient obtained from independent measurements (acceptor fluorescence intensity, anisotropy or lifetime data, “non-FRET” K_{pA}), and is affected by the fact that donors in one phase are sensitive to acceptors in the other, being closer to unity than the “non-FRET” value. This is useful for the purpose of estimation of domain sizes in this intermediate but potentially most relevant situation [33].

Alternatively, the approximate analytical solution recently derived by Towles et al. [37] can yield estimates of size of domains (taken as circular and with monodisperse size distribution) in biphasic systems. This approach requires the nontrivial input of radial distribution functions related to the probability of finding a domain at some distance of an average donor, for a system containing monodisperse domains of a given diameter. These two functions, one for donors inside and another for donors outside the domains, must be determined by numerical simulation. From these functions, ensemble averages of the acceptor density are calculated as a function of the distance to the donor. Ideally, the computation of the macroscopic donor decay would proceed by averaging over the decay kinetics of the donor ensemble, which is composed of an impossibly large number of non-equivalent donors, differing both in whether they are inside or outside the domains and, more crucially, in their location relative to the underlying domain structure, which determines the survival probability of each. Because this is unfeasible, the authors use a subtle approximation, treating all donors as equivalent (except only for their being either inside or outside a domain) and sensing a distance-dependent ensemble average acceptor density which is

calculated from the above mentioned radial distribution functions. That is, averaging is performed at the level of sensed acceptor density rather than at the level of survival rates of individual donors, which is reminiscent of the so-called “mean concentration model” [38,39]. The advantage of this necessarily complex and still approximate (but satisfactorily tested by analysis of numerically simulated decays, see below) model is that it yields the domain size as a fitting parameter. Indeed, if R_0 , the acceptor overall concentration, the fraction and area per lipid of each phase, all donor lifetime components, and both donor and acceptor partition coefficients are known, the decay at a given time is a (very complex, but this is certainly unavoidable) implicit function of the domain size. In practice, some of the input parameters may be calculated from independent measurements, whereas others may be constrained using global analysis. In a separate paper [34], the applicability of the formalism to polydisperse domains under different domain ordering regimes (hexagonal packing, totally random non-overlapping) was tested by comparison with numerical simulations (see below). It was concluded that the method was especially suited to probe the size of domains up to $4R_0$, with smaller relative uncertainty in this size range, regardless of domain polydispersity and packing. Confidence interval estimates are given as function of the recovered domain size/ R_0 ratio.

However, for the analysis of actual experimental results, these authors used a simpler model [40], which makes three simplifying assumptions: (1) donors are distributed randomly within the (cholesterol-rich) domain, (2) the domains are disklike, and (3) the domains are correlated across the bilayer leaflets (which is experimentally verified for compositionally symmetrical bilayers [5,41]). The FRET efficiency was calculated from the following expression [42]:

$$E = 1 - \frac{1}{\tau_0} \int_0^{\infty} \exp(-t/\tau_0) \exp[-n(S_1(t) + S_2(t))] dt \quad (13)$$

where

$$S_1(t) = \int_{LL1}^{\infty} \left\{ 1 - \exp\left[-(t/\tau_0)(R_0/R)^6\right] \right\} 2\pi r dr \quad (14)$$

refers to FRET within the same bilayer leaflet (*cis*), whereas

$$S_2(t) = \int_{LL2}^{\infty} \left\{ 1 - \exp\left[-(t/\tau_0)(R_0/R)^6\right] \right\} 2\pi r dr \quad (15)$$

reflects FRET between donors and acceptors in opposing leaflets (*trans*). The lower limits LL1 and LL2 in Eqs. 14–15 account for this difference. According to these authors, in a membrane system containing domains, two cases are possible: either both probes are located in the same phase, or the probes are located in opposite phases [40]. When both donor and acceptor are located in the same phase, LL1 is given by the sum of the molecular radii and LL2 is given by the bilayer thickness. If donor and acceptor are in different phases, then LL1 and LL2 become functions of domain radius. For the sake of averaging over the possible donor positions inside a circular domain, the authors take LL1 (closest approach distance between donor in domain and acceptor outside the domain) equal to 1/3 of the domain radius (because, for uniform distribution, the most probable distance to the center is 2/3 of the radius). LL2 is estimated from this LL1 value together with trivial geometric reasoning.

There are several limitations to this otherwise interesting model. First, it considers only two situations, donor and acceptor in the same continuous phase and in distinct (donor in the domains, acceptor outside the domains) phases. Therefore, the model does not consider the possibility of acceptors being located in domains (this can be minored by selecting an acceptor with no preference for the domains). A most important issue regarding this model is that it is only valid in the limit of infinite domain dilution. Otherwise, even disregarding the possibility of acceptors being located inside domains, the distribution function for donor–acceptor distance will

no longer be uniform, as there will be excluded areas. This is not accounted for in the model, because it assumes uniform distribution of acceptors, apart from the exclusion distances LL1 and LL2. The authors acknowledge this to some extent, by stating that the model is not valid for high l_0 (the domain phase in their assumption), before inaccurately claiming that such compositions are “not common biologically” [40]. Finally, whereas Eqs. 13–15 are used to calculate the FRET efficiency related to donors in the l_d (E_{same}) or l_o (E_{diff}) individual phases, these values are combined to produce the overall efficiency as an average,

$$E_{\text{overall}} = d_d E_{\text{same}} + d_o E_{\text{diff}} \quad (16)$$

weighed by the fraction of donors on l_d (d_d) and l_o (d_o) phases. This equation, however, is incorrect, as it can be readily shown that the true weights are the fractions of fluorescence light emitted by each of the subpopulations, not the molecular fractions. The effects of these limitations are hard to estimate, as no numerical simulation results are presented to test the formalism. Domain size studies using this treatment are described in Subsection 4.3. Strangely, no mention in this report is given to the more complex (but probably superior) formalism published previously in the same year by the same authors [37].

Gutierrez-Merino derived approximate analytical expressions for the average rate of FRET ($\langle k_T \rangle$) in membranes undergoing phase separation or protein aggregation [43,44]. Despite the simplicity and elegance of the model, it has found limited application, possibly due to underlying approximations (considering FRET only to neighboring acceptor molecules, and being based on the average rate of FRET, which is indirectly related to the experimental observable, the FRET efficiency).

Even more phenomenological treatments of FRET data can be useful in the detection of membrane heterogeneity. Silvius [45] described a FRET assay based on the measurement of the ratio of FRET efficiencies measured for two FRET pairs with a common acceptor. The FRET donors of the two pairs were chosen so that they had the same chromophore attached to the same location in the molecule, but showed preference for different phases. In the absence of domain formation, the FRET efficiency reported by both pairs is identical and the ratio is essentially unity. Phase separation leads to a decrease in the efficiency of the pair for which donor and acceptor have different phase preference, and conversely for the other pair. The ratio between the efficiency measured in the former and the latter pairs will be consequently less than unity. Applications of this assay are described in Subsection 4.3.

An alternative to approximate analytical solutions is the explicit computation of donor decay using numerical simulation. Snyder and Freire [46] calculated FRET efficiency curves as a function of acceptor concentration in this way for uniform and non-uniform (resulting from a heuristic potential function) probe distribution, and fitted their numerical results to simple analytical expressions, which can be conveniently used to analyze experimental data. Numerical simulations are also useful to provide tests for approximate analytical models of FRET with non-uniform chromophore distribution [33,37,47].

A special case of non-uniform distribution which has generated interest in membrane studies is the preferential location of certain lipids around a protein (in the so-called annular region). This type of lipid distribution heterogeneity will not be further described here, and the reader is referred to the original publications [48–50].

4. Applications

In this section we describe recent applications of FRET to membrane domain detection and characterization. Table 1 summarizes most of these studies carried out in model systems, listing them according to problem, FRET methodology and studied system.

Table 1
Summary of recent literature applications of FRET to the study of domain formation in membrane model systems

Application	Technique	System	References
Simple detection of heterogeneity	SS-FRET	bSM/Chol (so/lo),	[45]
		bSM/18:1,18:1 PC/Chol,	
		bSM/18:0,18:1 PC/Chol,	
		bSM/18:0,18:2 PC/Chol,	
		14:0,14:0/18:1,18:1/Chol,	
		16:0,16:0/18:1,18:1/Chol (ld/lo),	
		18:1,18:1 PC/Chol,	
		18:0,18:1/18:1,18:1/Chol (no domains detected)	
		14:0,14:0 PC/Chol (ld/lo)	[40]
		16:0,18:1 PC/PI(4,5)P ₂ (no domains detected)	[53]
Phase boundaries and probe partition coefficients	Theory+	14:0,14:0 PC/Chol (ld/lo)	[33]
	TR-FRET		
	Theory+	12:0,12:0 PC/16:0,16:0 PC (so/lo)	[35]
	SS-FRET	18:1,18:1 PC/16:0,16:0 PC/Chol (ld/lo)	[92]
Domain size estimation	TR-FRET+	14:0,14:0 PC/Chol (ld/lo)	[33]
	numerical simulation	Theory only	[33], [37], [43]
	TR-FRET	12:0,12:0 PC/18:0, 18:0 PC (so/ld)	[31]
		PSM/16:0,18:1 PC/Chol (lo/ld)	[88]
		16:0,18:1 PC/PCer (so/ld)	[64]
		16:0,18:1 PC/PSM/Chol (so/ld/lo)	
	SS-FRET+ Monte-Carlo	bSM/16:0,18:1 PC/Chol (ld/lo)	[90]
	SS-FRET	18:1,18:1 PC/16:0,16:0 PC/Chol (ld/lo)	[94]
Dynamics of phase separation	TR-FRET	12:0,12:0 PC/18:0, 18:0 PC (so/ld)	[6]

For each system, the type of heterogeneity is indicated. TR: time resolved. SS: steady-state. All other abbreviations are as used in the text.

4.1. One-phase lipid systems

Simple lipid systems without phase separation have been studied in the past, mainly for the purposes of comparison with theoretical formalisms [39,42,51]. At present, an important application of FRET is

as a test of whether the addition of a new component to a given one-phase lipid bilayer system induces compartmentalization and/or phase separation (which would be detected in the failure to analyze FRET kinetics with uniform probe distribution formalisms). In this vein, the possibility of clustering of phosphatidylinositol-(4,5)-bisphosphate (PI(4,5)P₂), a lipid implicated as regulator of several cellular functions and recently suggested [52] to segregate in a fluid PC matrix at or slightly above physiological pH without the contribution of any external agent (cholesterol or proteins), was investigated [53]. Time-resolved FRET between membrane probe 1,6-diphenylhexatriene (DPH) and 7-nitrobenz-2-oxa-1,3-diazol-4-yl (NBD)-labeled PI(4,5)P₂ in 16:0,18:1 PC vesicles with constant total PI(4,5)P₂ of 5 mol%, at pH 8.4, could be adequately described by Eq. 9 (Fig. 2). The recovered acceptor concentration values matched closely ($\pm 10\%$) the surface concentration expected from the partition coefficient determined for this lipid probe from variation of fluorescence intensity, therefore ruling out PI(4,5)P₂ clustering in these conditions. Additionally, the decrease of steady-state fluorescence anisotropy of NBD-PI(4,5)P₂ in 16:0,18:1 PC, which results from homo-FRET between labeled lipid molecules, is identical to that of 18:1,NBD-12:0 PC, an acyl-chain labeled PC uniformly distributed in 16:0,18:1 PC. The degree of energy migration of both lipid probes is almost identical (reflecting uniform distribution) and much smaller than for NBD-PI(4,5)P₂ in 16:0,16:0 PC at room temperature, where clustering is observed due to packing restraints in the 16:0,16:0 PC gel matrix (Fig. 2, inset). Together, the homo- and hetero-FRET experiments show that in the studied conditions, NBD-PI(4,5)P₂ clusters in gel membranes but not in fluid state bilayers. In this study [53], the previous erroneous detection of phase separation reported in the literature [52] was explained on the basis of the previous lack of quantification of partition of the NBD-PI(4,5)P₂ probe to the lipid vesicles.

In a similar manner, a specific interaction between the Trp-anchor of a series of transmembrane peptides with cholesterol was ruled out, since a random distribution of donor (Trp residue) and acceptor (dehydroergosterol, DHE) was proven in a fluid bilayer in the presence and absence of small amounts of cholesterol, i.e., in the ld phase [54]. At variance, in a mixture of 16:0,18:1 PC with cholesterol in the lo phase, the FRET efficiency between the Trp residue in the γ M4

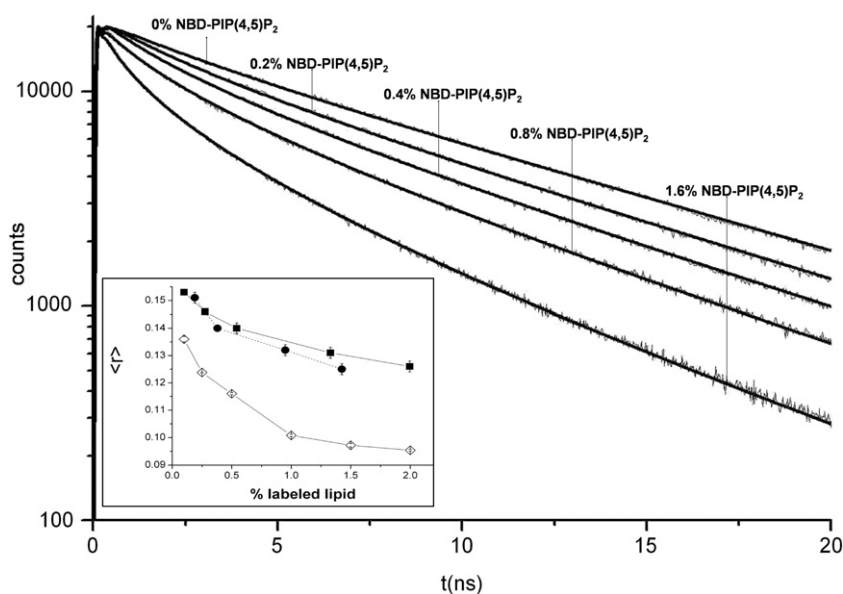


Fig. 2. Fluorescence decays of DPH in the absence and in the presence of increasing concentrations of NBD-PI(4,5)P₂ in 16:0,18:1 PC bilayers at pH 8.4 (thin lines). Global analysis of the data according to the model for homogeneous distribution of NBD-PI(4,5)P₂ (Eq. 3) resulted in the fitted curves (thick lines). Concentration of PI(4,5)P₂ was kept constant (5%) by addition of unlabeled PI(4,5)P₂. [Lipid]_{total} = 0.2 μ M. Inset: Fluorescence anisotropy of NBD-PI(4,5)P₂ in 16:0,18:1 PC (●) and 16:0,16:0 PC bilayers (◇), and of 18:1,NBD-12:0 PC in 16:0,18:1 PC (■). All measurements were performed at pH 8.4. [Lipid]_{total} = 0.2 μ M. Adapted from [52].

transmembrane domain of the nicotinic acetylcholine receptor was much lower than the value predicted for a random distribution of donors and acceptors [55]. Since from an independent method it was shown that the presence of peptide was not changing the phase behavior of the lipid mixtures, the FRET results could only be explained by considering the formation of peptide-enriched patches in the membrane, with a peptide area occupancy of ~30%, giving rise to a decreased acceptor (DHE) surface density near the donor peptide.

4.2. Binary phospholipid mixtures with gel/fluid phase separation

Gel/fluid phase separation has been studied extensively because it is easier from the technical point of view when compared to lo/ld phase separation. Here, we illustrate how time-resolved fluorescence spectroscopy and FRET can be used, knowing a priori the phase diagram, to obtain information regarding probe distribution, and domain size and dynamics. Recently, this type of lipid phase coexistence has gained renewed attention due to the increased cellular importance attributed to certain sphingolipids (e.g., [56]) with a very high main transition temperature (T_m), and the conviction that gel domains may form, albeit only transiently, on the plasma membrane of mammalian cells.

The binary phospholipid mixture 12:0,12:0 PC/18:0, 18:0 PC is well characterized from the equilibrium point of view, with a phase diagram showing a gel/gel and a very broad gel/fluid phase coexistence region [57]. Two different temperatures and compositions inside the gel/fluid phase coexistence range were chosen for a detailed FRET study [31] (circles in Fig. 1). The FRET donor used, *N*-NBD-12:0,12:0 phosphatidylethanolamine (PE), is short-tailed and prefers the fluid phase (rich in short-tailed lipid). For FRET acceptor, two molecules were used separately. The short-tailed 1,1'-didodecyl 3,3,3',3'-tetramethylindocarbocyanine (DiIC₁₂(3)) was shown to prefer the fluid phase from "non-FRET" K_p determination. The other studied FRET acceptor, long tailed probe 1,1'-dioctadecyl 3,3,3',3'-tetramethylindocarbocyanine (DiIC₁₈(3)), was expected to prefer the gel (rich in long-tailed phospholipid), and the partition coefficient obtained from fluorescence lifetime studies indeed indicated preferential partition of DiIC₁₈(3) into the gel. In this way, it was expected that phase separation would lead to an increased FRET efficiency inside a given tie-line for DiIC₁₂(3), because both donor and acceptor would be enriched in the same phase, whereas for DiIC₁₈(3) a decrease of FRET was expected due to segregation of donor and acceptor to different lipid phases. However, an increased FRET efficiency was observed in both cases, pointing to closer donor-acceptor proximity as a consequence of phase separation. These apparently conflicting results were rationalized on the basis of segregation of DiIC₁₈(3) to the interface between gel and fluid domains. Global analysis of donor's decays in the absence and presence of acceptor using Eq. 11 further corroborated this interpretation. In order for fluid-located donors to sense these interface-located acceptors, fluid domains should necessarily be small (not exceed ~10–15 nm). In a previous work, non-

random distribution of a similar carbocyanine acceptor probe in a pure gel phase had been shown [51]. The work in 12:0,12:0 PC/18:0, 18:0 PC shows that membrane probes which prefer the gel phase may show a non-random distribution in this medium, and tend to locate in an environment where favorable hydrophobic matching interactions occur but at the same time there are less packing constraints.

The dynamics of domain growth was also studied in the system 12:0,12:0 PC/18:0,18:0 PC (1:1 molar ratio) [6]. Large unilamellar vesicle suspensions were first equilibrated at 65 °C, a temperature above the T_m of both lipids, where the system is in the single fluid (supposedly homogeneous) phase situation. The lipid vesicles contain also a probe that partitions preferentially to the gel (*trans*-parinaric acid (*t*-PnA), with a gel/fluid $K_p=4.5$ as determined from fluorescence lifetimes, see also Table 2) and another that prefers the fluid phase (*N*-NBD-12:0,12:0 PE, used in the study described in the previous paragraph). Then, a sudden thermal quench to 20 °C is carried out, and the lipid mixture is rapidly taken to the gel/fluid phase coexistence region of the phase diagram (Fig. 1). The *t*-PnA to *N*-NBD-12:0,12:0 PE FRET efficiency (obtained from Eq. 3) as a function of time was measured and, as expected, it decreased, because as domains form and grow, due to the differential partition of the probes the donor is sensing a decreasing local concentration of acceptors. The process has a dynamics on the time-scale of hours. The trend of FRET efficiency with time could be well described by an exponential function with a non-zero value at infinite time ($E=0.19$). The calculated value considering infinite phase separation is also $E=0.19$. This shows that domains are, at least ~10 times R_0 , i.e., ~30 nm [33]. In the previous study, the domains were found to be smaller [31]. In that study, DiIC₁₈(3) was shown to be located mainly at the gel/fluid interface. In this way, the probe molecule would act as a surfactant, decreasing interfacial tension, and limiting the growth of the domains. In the non-equilibrium study [6], the result obtained indicates that *t*-PnA has a random distribution in the gel phase and is not affecting the interfacial tension between gel/fluid domains. In addition, the slow dynamics of phase separation ascertained the importance of interfacial phenomena previously pointed out by Monte-Carlo simulations of the equilibration process [58], that drew attention to the long equilibration times that may be necessary for equilibrium studies of this and other kinds of lipid mixtures.

Ceramide is the cellular precursor of sphingomyelin (SM), and can also be formed from SM at the cell surface, through the action of the enzyme sphingomyelinase, with marked effects on rafts and cell processes such as signal transduction (e.g., [59]). Numerous studies show that ceramide production in response to external stress stimuli is a nearly universal feature of programmed cell death (for reviews see [60,61]). Evidence is emerging for the indirect action of ceramide, resulting from the alterations of the biophysical properties of the plasma membrane [62,63]. To understand the role of ceramide in signal initiation and lipid second-messenger formation from rafts, it is necessary to systematically characterize the changes that occur at the plasma membrane upon increase in ceramide level.

Table 2

Partition coefficients of the probes between lo and ld, $K_p^{lo/ld}$, gel and fluid, $K_p^{g/f}$, and gel and gel, $K_p^{g/g}$, phases

Probe	$K_p^{lo/ld}$ in 16:0,18:1 PC/Chol	$K_p^{lo/ld}$ in 16:0,18:1 PC/PSM/Chol	$K_p^{g/f}$ in 16:0,18:1 PC/PSM	$K_p^{g/f}$ in 16:0,18:1 PC/PCer	$K_p^{g/g}$ in PCer/PSM
DPH	~1 ^a	1.05±0.08 ^c	~1 ^a	~0 ^{c,g}	~0 ^d
NBD-18:1,18:1 PE	–	1.20±0.06 ^c	–	~0 ^{c,g}	–
NBD-16:0,16:0 PE	–	3.7±0.5 ^c	–	~0 ^{c,g}	–
Rho-18:1,18:1 PE	0.7±0.2 ^b	0.28±0.08 ^c	–	~0 ^{c,g}	–
<i>t</i> -PnA	0.8±0.2 ^c	0.88±0.05 ^c	1.9±0.1 ^d	4.50±0.60 ^f	2.4±0.4 ^d

^a [76].

^b unpublished.

^c [89].

^d [104].

^e [55].

^f [64].

^g The photophysical parameters of these probes remain almost unchanged with PCer-gel fraction indicating that their partition into the PCer-gel phase is very low.

In order to address these aspects, we first selected a binary system and systematically studied the effect of increasing amounts of *N*-16:0-ceramide (PCer) on the properties of 16:0,18:1 PC bilayers [64], before characterizing the interplay of Cer with lipid rafts, in more complex lipid mixtures (see Subsection 4.4). The complete description of the 16:0,18:1 PC/PCer lamellar phases was possible because three probes with different lipid-phase related properties were employed: *t*-PnA which partitions preferentially to gel phases [6,65]; DPH, which is expected to distribute equally between phases [66,67]; and *N*-NBD-18:1,18:1 PE, a phospholipid with unsaturated acyl chains and the fluorescent label in the head-group, preferring fluid rather than gel lipid phases (see [68], and references above). Comparing the behavior of the probes [64] (Table 2), it can be concluded that whilst *t*-PnA partitions to PCer-gel domains and thus is able to follow PCer domain formation and report their properties, DPH is excluded from these domains. Moreover, since usually the partition coefficient is $K_p \sim 1$ for DPH in a typical gel–fluid separation, the ceramide-rich gel domains should be highly ordered and compact, in order to exclude the probe. On the other hand, the head-labeled lipid *N*-NBD-18:1,18:1 PE is the only probe among those three that is able to detect a transition of PCer gel phase at room and physiological temperature (from which it is excluded) to another type of gel, where dehydration and increased rigidity at the head-group membrane/water interface sensed by the headgroup fluorophore occurs. A complete temperature/composition 16:0,18:1 PC/PCer phase diagram was constructed [64]. After the phase diagram determination, the FRET methodology along a tie-line described in the previous section could be applied. The pair used was the *t*-PnA/*N*-NBD-18:1,18:1 PE for which the photophysical properties and the partition coefficients were determined during the phase diagram determination. In the present case, FRET efficiency from *t*-PnA to *N*-NBD-18:1,18:1 PE decreased steeply from the random value in the fluid to a value close to zero for >50 mol% of gel, due to the exclusion of *N*-NBD-18:1,18:1 PE from the PCer enriched gel phase, which is the one where most of the donor's fluorescence comes from, due not only to a preferential partition of *t*-PnA into those domains but also to a several-fold higher quantum yield in that phase than in 16:0,18:1 PC-enriched fluid phase. Thus, the ceramide-rich domains reach the infinite phase separation limit readily, and PCer-enriched domains were estimated to be larger than ~60 nm [64]. Studies in more complex (raft-like) systems containing Cer are described in Section 4.4.

4.3. *ld/lo* phase separation

PC/cholesterol (Chol) binary systems are among the most studied lipid mixtures of the previous three decades. As discussed in section 1, it is well documented and generally recognized that in the presence of high amounts of Chol in a PC bilayer, the membrane is in a liquid ordered (*lo*) phase (using the nomenclature introduced in [3]) with intermediate properties between those of the gel and the fluid. In this nomenclature, the gel and fluid phases are designated by solid ordered (*so*) and liquid disordered (*ld*), respectively. Most reported phase diagrams are monotectic, including those of the 16:0,16:0 PC/Chol [3,69–72], 14:0,14:0 PC/Chol [73,74], 16:0,18:1 PC/Chol [74–78] and SM/Chol [76,79–81] mixtures. Below the monotectic temperature (close to T_m), *so/lo* coexistence occurs for intermediate cholesterol concentrations, whereas this applies to *ld* and *lo* phases above the monotectic temperature.

The FRET formalism described in Section 3 was applied to mixed 14:0,14:0 PC/Chol large unilamellar vesicles [33]. Three compositions inside the phase coexistence range ($x_{\text{chol}}=0.15, 0.20$ and 0.25) were studied at two $T > T_m$ values ($T=30$ °C and $T=40$ °C), by FRET between *N*-NBD-14:0,14:0 PE and *N*-(lissamine-rhodamine B) (Rh)-14:0,14:0 PE. “Non-FRET” distance-independent *lo/ld* partition coefficients were obtained for donor (from variation of fluorescence anisotropy) and acceptor (from variation of fluorescence intensity). These pointed to

preference of the donor for the *lo* phase and preference of the acceptor for the *ld* phase. Therefore, it was expected that phase separation led to a decrease in FRET efficiency, as it would cause an average increase in donor–acceptor distance. This was indeed verified, and the observed decrease is more pronounced for higher *lo* fraction than lower *lo* fraction. On the other hand, it was found that the acceptor concentrations recovered from the fits to donor fluorescence decays were higher than expected for the *lo* phase and lower than expected for the *ld* phase (leading to a FRET K_p closer to unity for the acceptor) near the *ld* phase boundary. This was not verified at the other end of the phase coexistence range. All these observations indicated that the *lo* domains dispersed in a majority *ld* phase were small (<3–5 R_0 , or 18–30 nm), contrary to the *ld* domains dispersed in a majority *lo* phase (>5 R_0 , or ~30 nm).

Brown et al. [40] applied their formalism (see Section 3) to FRET between donor DHE and acceptor 2-[12-[(5-dimethylamino-1-naphthalenesulfonyl)amino]dodecanoyl] PC (DANSYL-PC) to demonstrate domain formation in the same lipid system. Whereas the *lo/ld* partition coefficient of DHE was assumed to be equal to that of Chol (readily available from the phase diagram), the acceptor was assumed to display complete preference for the disordered phase (as required in the authors' model [40]), from the variation of DANSYL-PC emission maximum as a function of cholesterol content. No domain sizes, however, were inferred for this mixture.

Silvius [45], using the assay described above (see Section 3), detected domain formation in the binary system Brain SM (bSM)/Chol (*so/lo* coexistence) with NBD tetraacyl (either saturated or unsaturated) donors and *N*-Rh-diphytanoyl-PE as acceptor, but not in 18:1,18:1 PC/Chol (for which phase separation has indeed never been reported in the literature – see [82]).

The most actively studied type of lipid domains is known as lipid rafts, which are thought to consist of sphingolipid and Chol-enriched and (unsaturated) PC-depleted domains. Rafts in a rest state in cell membranes seem to be in general <100 nm (e.g., [83–86]), in the size range accessible by FRET. The simplest model for rafts is a mixture of a high transition temperature (T_m) lipid (usually a saturated PC or SM) with a low T_m lipid and cholesterol. The rafts would correspond to the *lo* domains high T_m lipid- and cholesterol-enriched, in an *ld* low T_m lipid-enriched matrix.

Silvius [45] detected inhomogeneity in lipid organization in bSM/18:1,18:1 PC/Chol at 20 °C, 30 °C and 37 °C for 33 mol% of the latter component. Whereas fluorescence microscopy studies had already revealed micron-size domains in systems composed of SM, Chol and an unsaturated PC at room temperature, this structure was not apparent at physiological temperatures [12,87]. The fact that FRET sensed inhomogeneous probe distribution in these conditions was indicative of the formation of domains of at least the order of R_0 . The assay even detected inhomogeneity in the same mixture for 50 mol% of Chol at 37 °C, as well as in systems which had the PC with saturated *sn*-1 and unsaturated *sn*-2 acyl chains (a common motif found in naturally occurring phospholipids) such as bSM/18:0,18:1 PC/Chol and bSM/18:0,18:2 PC/Chol (33 mol% Chol, 20 °C), and in systems with bSM replaced by a doubly saturated PC such as 14:0,14:0/18:1,18:1/Chol or 16:0,16:0/18:1,18:1/Chol (33 mol% and 50 mol% Chol, 20 °C, in both cases), but not with two PCs with unsaturated chains, such as 18:0,18:1/18:1,18:1/Chol.

Another system in which the PC component has one saturated acyl chain and the other one unsaturated is the arguably archetypical raft model ternary system, palmitoyl SM (PSM)/16:0,18:1 PC (the major lipid component in PC isolated from several natural sources; [2])/Chol. This system was investigated to see if the interesting composition dependence of domain size observed for 14:0,14:0 PC/Chol [33] could be observed for this more complex (and more biologically relevant) system. Contrary to the binary mixture, the phase diagram for the ternary system was previously unknown. As explained in Section 3, the use of FRET for domain size estimation requires the knowledge of

the phase boundaries, and FRET measurements should be carried out along a tie-line, so that the composition of each phase does not vary.

For this purpose, the PSM/16:0,18:1 PC/Chol phase diagram was determined at room temperature (and a reasonable expectation for 37 °C was proposed) using photophysical, domain size-independent techniques [76]. Briefly, the three binary phase diagrams were firstly determined. The PSM/16:0,18:1 PC binary phase diagram was obtained from the variations of steady-state fluorescence anisotropy of DPH. The PSM/Chol phase diagram was obtained using this same technique above the T_m of PSM, and quenching of DPH fluorescence by 5-doxyl stearic acid (5-NS) below that temperature, together with the amplitudes of the fluorescence lifetime components of DPH. Finally, the 16:0,18:1 PC/Chol ld/lo phase boundaries were determined in the 15–40 °C temperature range, using steady-state fluorescence anisotropy of DPH and fluorescence lifetime of *t*-PnA. Selected points in the ld/lo and lo/gel (so) boundary lines for ternary mixtures at room temperature were then obtained, using fluorescence anisotropy of DPH for the former and quenching of this probe's fluorescence by 5-NS for the latter. Based on the phase boundaries experimentally determined and restrictions imposed by thermodynamic reasoning, estimates for the phase compositions along the tie-line containing the often-used 1:1:1 composition were obtained at both 23 °C and 37 °C. The tie-lines obtained agreed well with all the literature and were later confirmed from the trend of variation of the photophysical properties of several fluorescent membrane probes [88,89].

Taking into consideration the preceding study of the 14:0,14:0 PC/Chol system [33], the chosen probes for the FRET study in the ternary mixture were *N*-NBD-16:0,16:0 PE as donor and *N*-Rh-18:1,18:1 as acceptor [88]. Like their counterparts in the binary system, the donor probe was found to have selectivity for the lo phase, whereas the opposite was verified for the acceptor, using domain size-independent methods. Therefore, in the phase coexistence region it was expected that energy transfer were less efficient than for pure ld and lo phases. As shown in Fig. 3, this is indeed the case. The FRET efficiency decreases from the value measured for pure ld as a consequence of phase separation, before rising again near the high-Chol end of the tie-

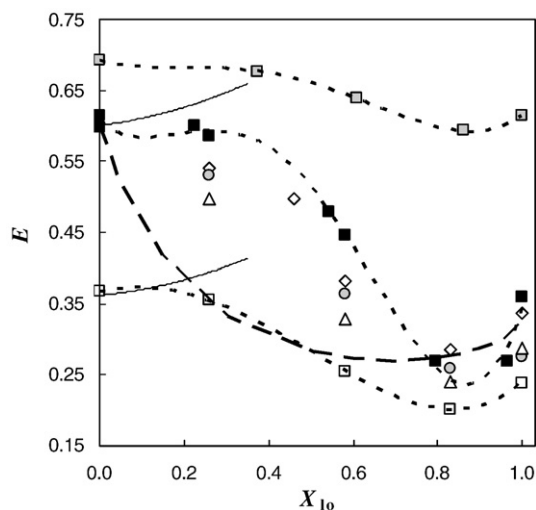


Fig. 3. Variation of E of the donor/acceptor pair *N*-NBD-16:0,16:0 PE/*N*-Rh-18:1,18:1 PE in PSM/16:0,18:1 PC/Chol large unilamellar vesicles, as a function of the lo fraction (X_{lo}), along the tie-line containing the 1:1:1 mixture. The dotted lines are merely guides to the eye. The thin solid lines are the values of E calculated for a random distribution of donor and acceptor molecules in pure ld phase for acceptor/lipid ratios of 1:200 and 1:500. The different data sets correspond to 1:200 acceptor lipid ratio, with 0 mol% G_{M1} and 2 mol% G_{M1} /no CTB indistinguishable (■), 2 mol% G_{M1} and excess CTB (◇), 4 mol% G_{M1} and no CTB (●), 4 mol% G_{M1} and excess CTB (△); 1:500 acceptor lipid ratio, with 0 mol% G_{M1} (□). For comparison, the values for the binary system DMPC/chol along the ld/lo tie-line at 30 °C are also shown (■) [34]. The theoretical line for infinite phase separation (large domains), for the 1:200 acceptor/total lipid mole ratio is also shown (dashed line). Adapted from [87].

line. The figure shows several data sets: acceptor:lipid mole ratios of 1:200 and 1:500 for the PSM/16:0,18:1 PC/Chol system, and, for the sake of comparison, acceptor:lipid mole ratio of 1:200 for the 14:0,14:0 PC/Chol system study described above.

The curves are qualitatively very similar, showing that a significant drop in FRET efficiency only occurs for lo fraction ≈ 0.35 . This is in contrast with the theoretical curve assuming infinite phase separation (large domains), for which a steep drop was expected already for very low lo fraction. Thus, domains in the low lo fraction range, while definitely forming (in the absence of phase separation, E would actually increase due to the cholesterol condensing effect, as apparent on the thin lines in Fig. 3), are very small. On the other hand, the theoretical curve for infinite phase separation describes well the experimental data for high lo phase fraction. There is also qualitative agreement with the data from the 14:0,14:0/Chol binary system at 30 °C [33]. However, the magnitude of the FRET efficiency drop is much higher in the ternary system, indicating that phase separation is more pronounced in the latter. In this study it was also observed that the raft marker ganglioside G_{M1} in small amounts (and excess cholera toxin subunit B, CTB) does not affect the general phase behaviour of the lipid system, but can increase the size of the rafts on the low liquid ordered, small to intermediate domain region. This is concluded from the drop in E for the samples with 4 mol% G_{M1} , with or without excess CTB, or 2 mol% G_{M1} , only with excess cholera toxin subunit B for this composition range (Fig. 3). The phase diagram is shown in Fig. 4. An upper limit of 20 nm can be given for the lo domains (rafts) when these represent less than 35 mol%, from numerical simulations [33].

A very similar system, bSM/16:0,18:1 PC/Chol, was studied using a combination of FRET (between 1-[[[(6,8-difluoro-7-hydroxy-4-methyl-2-oxo-2H-1-benzopyran-3-yl)acetyl]oxy]-(Marina Blue-)] and *N*-NBD-16:0,18:1 PE) and lattice Monte-Carlo simulations [90]. For the purpose of FRET efficiency calculation from the simulations, the actual distance dependence of the FRET interaction (given by rearranging Eq. 5) was replaced by a step function, meaning that FRET was considered to occur if the donor–acceptor distance in a given pair is less than R_0 (4.6 nm), that is 6 lipid molecules in the same lattice (leaflet) or 2 in the opposite one. In the Monte-Carlo simulations, the authors used unlike nearest-neighbor interaction parameters based on experimental data and fine-tuned to match the experimental FRET. These were the only potential fitting parameters in their calculations. Using this methodology, the authors were able to observe extensive phase separation for SM/Chol/16:0,18:1 PC mole ratio 35:35:30. This agrees with the results of de Almeida et al. [88] described above, which indicate the existence of large ld domains in this lo-rich area of the phase coexistence range. No extensive phase separation is observed in the Monte-Carlo simulation of either of the binary mixtures SM/16:0,18:1 PC 70:30, Chol/16:0,18:1 PC 70:30 or SM/Chol 50:50, which, as argued by the authors, agrees with the lack of observation by fluorescence microscopy in giant unilamellar vesicles of micron-scale phase separation in the binary SM/Chol, SM/16:0,18:1 PC, and Chol/16:0,18:1 PC systems, unlike some ternary mixtures of these components. According to the authors, these results also support the existence of a “closed loop” for ld/lo coexistence [90], as proposed by them in an earlier report [91]. However, although the existence of a closed loop excludes ld/lo phase separation in the binary 16:0,18:1 PC/Chol system, as observed by de Almeida et al. [76], the fact is that all three binary systems mentioned above happen to lie in one-phase regions of the diagram proposed by the latter authors [76], and thus do not directly contradict it. In any case, the work of Frazier et al. [90] shows that FRET and computational techniques can be used to create a powerful combination, suited to the study of lipid phase separation.

The SP-FRET methodology introduced in Section 3 was applied to estimation of phase boundaries in the 18:1,18:1 PC/16:0,16:0 PC/Chol system at 25 °C, 35 °C and 45 °C [92]. In this study, no tie-lines are reported, and the equilibrium lines are obtained from variation of sensitized emission of 3,3'-dioctadecyloxycarbocyanine (18:0-DiO)

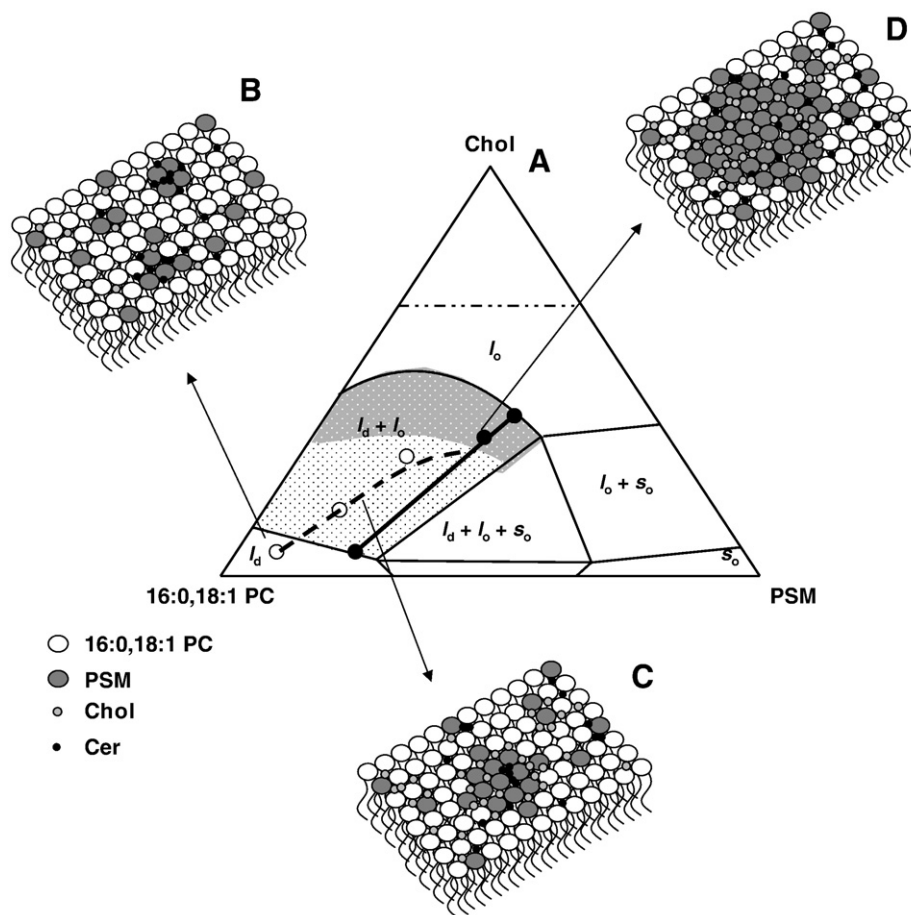


Fig. 4. Schematic representation of the effect of PCer in lipid rafts biophysical properties and organization. 16:0,16:1 PC (A) By recruiting PSM, PCer changes the composition of the mixtures and consequently the position of the tie-line of the remaining fluid phase. The dashed black line and the white dots correspond to the estimated composition of the fluid phase that remains after the sequestering of PSM for gel-domain formation. When increasing Chol content, the effect of PCer is opposed and less PSM is recruited for domain formation until 25%–33% Chol is reached and gel-domain formation completely abolished. Thus, the line that defines fluid phase composition should connect with the tie line in this region. According to this model, X_{l_o} should decrease from 26% and 58% to 21% and 54%, respectively, when 4% PCer is present. (B) For the 100% l_d phase one PCer molecule recruits up to three PSM molecules and forms highly ordered PCer/PSM-gel domains. The amount of gel formed is considerable, $X_G \sim 15\%$, but the size of the domains is small, ~ 4 nm. Panels B, C, and D are a pictorial top view of the bilayer because ~ 250 molecules should be involved in the formation of a nanodomain of this dimension. (C) In the low-to-intermediate Chol mole fraction range, i.e., in the range of small sized rafts, PCer/PSM-gel domains are still present and are surrounded by lipid rafts (l_o phase). FRET experiments show that PCer is not forming platforms or promoting the coalescence of the small rafts into large ones. (D) In the high Chol, large sized rafts range, PCer ability to form gel domains with PSM is abolished by the presence of Chol that competes for the association with PSM. In this situation, lipid rafts are governing membrane properties. Adapted from [88].

acceptor, using DHE as donor (R_0 between 2.0 and 3.6 nm), measured for 1294 independently prepared samples. Whereas the overall shape of the diagram is similar to that reported from confocal fluorescence microscopy and solid-state NMR studies [12,93] important differences are found. Notably, the l_o/l_d coexistence range is much narrower at room temperature (not extending beyond 33 mol% Chol, compared to 50 mol% for the confocal fluorescence microscopy boundary), and this range shifts in its entirety to higher 16:0,16:0 PC contents as the temperature increases, whereas the reported confocal fluorescence microscopy study only revealed shifting of the l_d boundary, with the l_o extreme remaining more or less invariant. Instead of attributing these conflicting results to differences in the techniques used, the authors suggest they may originate in differences in sample preparation, with techniques requiring film deposition during sample preparation (as e.g. required for giant unilamellar vesicle preparation) being prone to artifactual demixing of lipid components, contrary to the multilamellar dispersions prepared by rapid solvent exchange by the authors [92]. Interestingly, two other studies on this ternary system were published in the same year, neither of which restricted to giant unilamellar vesicles. De Almeida et al. [82], using a combined time-resolved fluorescence microspectroscopic approach (that is, fluorescence lifetime imaging microscopy and microscopic fluorescence decays measured in giant unilamellar vesicles, and macroscopic

fluorescence decays measured in large unilamellar vesicles) established the existence of the three-phase triangle near the 16:0, 16:0 corner, thus narrowing the l_d/l_o range previously reported [93]. On the other hand, an NMR study with multilamellar vesicles [19] indicated that the l_o/l_d coexistence range does not extend beyond 35 mol% Chol in the 10–37 °C range.

The same ternary mixture was studied by Brown et al. [94] using their above described formalism [40] (modified to allow the introduction of polydispersity in domain size) with the same FRET pair (DHE/DANSYL-PC). Contrary to the study of Buboltz et al. [92], the authors propose an extension of the two-phase region of this mixture, to include e.g. the mole composition 18:1,18:1 PC/16:0,16:0 PC/Chol 2:1:2. This opposite behavior is possibly due to the enhanced sensitivity of this method for small domains, whereas the phase boundaries of Buboltz et al. [92] are obtained only in the infinite phase limit. However, the application of the formalism to data points closer to the l_o boundary (up to 0.7–0.8 of l_o mole fraction) is, as commented above, incorrect. Therefore, and taking into view all other simplifications in these authors' model, the size determinations, mapped over the phase diagram, must be viewed with caution. The authors also studied the 16:0,18:1 PC/16:0,16:0 PC/Chol system, where no extensive phase separation is detected, including in the sample with 16:0,18:1 PC/Chol 4:1 mole ratio [94]. In fact, whereas this

composition lies just inside the phase coexistence of the 16:0,18:1 PC/Chol binary system [76], the domains therein are expected to be too small for even FRET to detect [88]. Recently, thorough molecular dynamics simulations revealed interesting details on the molecular interactions of lipids with different degrees of unsaturation and cholesterol, that may lead to a further understanding of the complex behaviour of these systems [95].

Phase separation in fluid mixed bilayers can also be induced by the presence of proteins and FRET can be used for its detection. Fernandes et al. [96] found that FRET between *N*-(iodoacetyl) aminoethyl-1-sulfonaphthylamine (AEDANS)- and *N*-(4,4-difluoro-5,7-dimethyl-4-bora-3a,4a-diaza-s-indacene-3-yl)methyl (BODIPY)-labeled M13 bacteriophage major coat protein followed the expected FRET kinetics for uniform fluorophore distribution in 18:1,18:1 PC/18:1,18:1 phosphatidylglycerol (PG; 4:1 mole ratio) and 18:1,18:1 PE/18:1,18:1 PG (7:3) bilayers (meaning that protein distribution remained uniform in these three systems, and its incorporation did not lead to phase separation in the latter two mixed bilayers), at variance with the behavior observed for 22:1,22:1 PC/18:1,18:1 PC (3:2) and 14:1,14:1 PC/18:1,18:1 PC (3:2). In these latter systems, enhanced FRET was attributed to phase separation, probably induced by the protein, which is preferably located in the domains enriched in the hydrophobic matching lipid (18:1,18:1 PC).

4.4. Gel/ld/lo phase separation

From the biophysical point of view, ceramide (Cer) became a key molecule due to its ability to drive gel/fluid phase separation in biologically relevant conditions. As shown above, long chain ceramides are able to segregate into gel domains in 2-component model membranes containing either fluid [64,97–101] or gel phase lipids [102,103]. However, in more complex systems the effects of Cer in both membrane physical properties and lipid lateral organization are not so straightforward. For instance, whereas in membranes containing SM and a fluid lipid, Cer can drive the formation of one SM/Cer- or two SM- and Cer-enriched gel phases [104], in membranes containing Chol, Cer-ability to segregate into gel domains is highly dependent on the amount of Chol present [89]. Therefore, studies of Cer effects in raft mimicking membranes are highly relevant, not only because of the biological relevance of lipid rafts (as discussed in the previous subsection), but also because these domains are the primary site of action of the enzyme sphingomyelinase (SMase), that catalyses the hydrolysis of SM into Cer [105].

Due to the inherent experimental complexity of studies involving Cer (e.g. [62]), only a small number of works are focused on the study of Cer effects on raft membranes. Important information was obtained from atomic force microscopy (AFM) [106,107], AFM coupled with fluorescence correlation spectroscopy (FCS) [108] or by fluorescence spectroscopy [89]. AFM is very advantageous because it gives direct visual information on phase separation. However, the nature of the phases present can only be predicted indirectly by the height difference. Coupling FCS to AFM gives additional information regarding the diffusion of the lipids. The application of these techniques to the study of Cer effects on raft membranes allowed concluding that Cer segregates into a distinct phase, most likely a gel-like phase. These Cer-enriched domains are mainly located at the boundaries or inside SM-rich domains [106–108]. It was also suggested that Cer is able to increase the order of the fluid phase and to drive coexistence of three phases under certain lipid compositions [108]. However, with these studies it was not possible to unambiguously elucidate the nature and lipid composition of the phases.

To answer those questions, the application of the multiprobe fluorescence approach (Subsection 4.2) together with FRET methods was valuable [89]. This methodology was applied by us to study the effect of Cer on 16:0,18:1 PC/PSM/Chol raft mixtures presenting different lipid composition (Fig. 4) [89]. The combination of five

different fluorescent probes (Table 2) was required for full characterization of the phases formed, because 2 or 3 phases are coexisting, depending on the lipid composition of the raft mixtures. For example, *t*-PnA fluorescence anisotropy and mean fluorescence lifetime were valuable to detect the formation of Cer-gel phase, which only occurs in raft mixtures with low Chol content (as schematically represented in Fig. 4), [64,89]. On the other hand, the combination of information obtained with all the other probes was essential to establish the presence of lo and ld phases [89].

Beside the information about the number and nature of the phases present in the mixtures, additional details regarding amount and composition of the gel phase formed is directly obtained through the application of formalisms that allow quantifying the gel formed according to the variation of the photophysical parameters of the probes, namely the mean fluorescence lifetime of *t*-PnA (see Eq. 2 in [89]). This allowed concluding that in the low Chol range, low Cer amount (4 mol%) is able to recruit SM to form ~15% gel phase, i.e., each Cer molecule recruits up to 2-to-3 SM molecules to form a highly-ordered and compact Cer/SM-enriched gel phase (Fig. 4). This model is further validated by measuring FRET among *N*-Rh-18:1,18:1 PE molecules, i.e., homo-FRET. This probe is excluded from Cer-gel domains (Table 2) and, therefore, when these domains are formed the surface area for probe distribution decreases. Due to the small Stokes shift of *N*-Rh-18:1,18:1 PE, energy migration occurs, which is reflected in a decrease in the anisotropy of the probe. The application of Snyder and Freire model [46], which predicts the depolarization of Rh as a function of the surface density of the probe, allows rationalizing the variation in the anisotropy and estimate the area involved in gel domain formation. It was concluded that an area reduction of ~5.1 Å² was required to account for the observed depolarization, and this value was similar to the one calculated assuming that 11% SM and 4% Cer were involved in the formation of the gel phase (~5.2 Å²).

The combination of the information obtained by the use of multiple donor/acceptor (D/A) FRET pairs, with distinct phase-related properties, is valuable to study the lipid lateral organization and domain size in complex systems, such as the one here presented [89]. To discriminate if Cer is able to induce the formation of the so-called Cer-platforms or the coalescence of small rafts, or if it forms small scattered gel domains, three D/A pairs were selected to obtaining information regarding i) ld/lo phase separation, i.e., alteration in lipid raft organization (D/A pair 1: *N*-NBD-16:0,16:0 PE/*N*-Rh-18:1,18:1 PE); ii) gel/lo phase separation, thus, the organization between the so-called Cer-platforms and lipid rafts (D/A pair 2: *t*-PnA/*N*-NBD-16:0,16:0 PE); iii) gel/fluid (ld+lo) phase separation (D/A pair 3: *t*-PnA/*N*-NBD-18:1,18:1 PE).

The variation of FRET efficiency for the *N*-NBD-16:0,16:0 PE/*N*-Rh-18:1,18:1 PE pair (D/A 1) in raft mixtures in the absence and presence of Cer further supported the ability of Cer to form gel domains only in the low Chol range. This is concluded from an increase in FRET efficiency when Cer is present in these mixtures due to the exclusion of both D and A from Cer-gel domains. Moreover, the application of the above described FRET formalisms showed that, 15% Cer/SM-enriched gel phase was, in fact, being formed in the mixtures with lowest Chol content, because the increase in the experimental FRET efficiency was identical to the one calculated for a situation where D/A randomly distribute (see Section 3 for FRET formalisms for random D/A distribution) in a fluid area that was reduced by ~5.2 Å² due to the formation of the referred gel phase fraction. This formalism also allows obtaining information about the organization of the raft domains. For instance, if Cer were able to induce raft coalescence then FRET efficiency should decrease because the separation distance between the acceptor and the donor would increase as a consequence of the different phase partition of these molecules (Table 2). This would be translated in a variation of FRET efficiency similar to the one reported for raft mixtures in the presence of G_{M1} and CTB (Fig. 3), which are able to promote raft coalescence to a significant extent [88].

On the contrary, in the presence of Cer, and in the low Chol range, FRET increased, undoubtedly showing the inability of Cer to induce the coalescence of raft domains.

Additional topological information of this complex system is obtained with the two other D/A pairs, namely the size of the gel domains. Because *t*-PnA (donor) has a strong preference towards Cer-enriched gel phases, while both acceptors (*N*-NBD-16:0,16:0 PE and *N*-NBD-18:1,18:1 PE) are excluded, when gel domains are formed FRET efficiency decreases (Fig. 5). Once again, this was observed for Cer-containing raft mixtures in the low Chol range. Because the acceptors are completely excluded from Cer-gel domains it is possible to estimate their size through the application of the FRET formalisms that take into account the existence of phase separation (see Section 3, in particular Eq. 11). In this particular case, it has to be considered that: i) FRET within gel phase does not occur because A are excluded; ii) there is FRET from the gel to the fluid phase; iii) FRET occurs within the fluid phase. Furthermore, it is necessary to take into account the concentration of the donor in each of the phases (determined according to its partition coefficient), the amount of gel phase formed

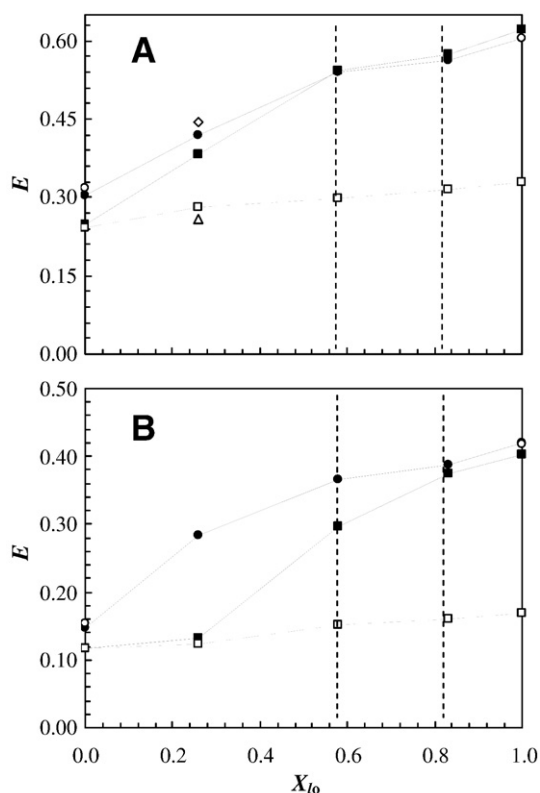


Fig. 5. Variation of FRET efficiency, E , for the D/A pairs (A) *t*-PnA/*N*-NBD-16:0, 16:0 PE (D/A 2), and (B) *t*-PnA/*N*-NBD-18:1, 18:1 PE (D/A 3) as a function of X_{lo} in the l_o/l_d coexistence region along the tie line of the ternary phase diagram for the 16:0,18:1 PC/PSM/Chol mixture [75] containing 0 (circles) and 4 (squares) mol% PCer. Experimental data are represented by solid symbols, and open symbols are values from theoretical calculations. The open circles were obtained by calculation of the expected E for a random distribution of donors and acceptors. The open squares correspond to the expected E when donors located both in the gel and fluid phases are transferring energy to acceptors randomly distributed in the fluid phases. In these calculations a gel phase mole fraction X_G equal to 15% and $R_e = 3.8$ and 4.0 nm for *N*-NBD-16:0,16:0 PE and *N*-NBD-18:1, 18:1 PE, respectively, were assumed. The open triangle and the open diamond (A) correspond to the expected E for a situation where PCer/PSM gel domains are surrounded by only l_d or l_o phases, respectively. It was assumed that donors located in the gel phase were only able to transfer to one of the fluid phases, $X_G = 15\%$, $R_e = 3.8$ nm, and the amount of donor in the gel phase and the surface density of the acceptors in each fluid phase was taken into account. The dotted and dotted-dashed lines are only to guide the eye. The vertical dashed lines correspond to the mixtures containing 25% and 33% Chol. Time-resolved FRET measurements are extremely reproducible, and variations in the values of E are within <1.5% for completely independent samples. Adapted from [88].

and the existence of an exclusion distance, R_e , between D and A for FRET from the gel to the fluid phase. The size of the domains is then given by the R_e value that is required to obtain a FRET efficiency identical to the one determined experimentally. The application of this formalism to both D/A pair yielded the same conclusions: Cer associates with SM to form small, ~ 4 nm, gel domains (Figs. 4–5).

Another advantage of using multiple FRET pairs is the capacity to obtain information regarding the lateral organization of the fluid phases around the gel domains. For instance, taking benefit of the different partition of the acceptors in the *t*-PnA/*N*-NBD-16:0,16:0 PE (D/A 2) and *t*-PnA/*N*-NBD-18:1,18:1 PE (D/A 3) D/A pairs it was shown that Cer/SM-enriched gel domains were surrounded by l_o phase. This is detected in a qualitative way by direct inspection of the different variation of FRET efficiency for both D/A pairs: FRET efficiency is higher when *N*-NBD-16:0,16:0 PE is used as an acceptor (D/A 2) showing that l_o phase must be closer to Cer-gel domains (Fig. 5). This is because this acceptor presents a strong partition into l_o phase, while the other acceptor (*N*-NBD-18:1,18:1 PE) shown an even partition between the two fluid phases. If FRET is higher for D/A 2 compared to the *t*-PnA/*N*-NBD-18:1,18:1 PE D/A 3 pair this means that in the former situation the acceptors are located closer to the donor, and therefore l_o phase is in the vicinity of gel phase. This is further corroborated from a quantitative point of view, through the calculation of the FRET efficiency expected for the D/A 2 pair in a situation where a) only l_d phase is surrounding Cer/SM-enriched gel domains and b) only l_o phase is surrounding Cer/SM-enriched gel domains. The FRET formalisms applied to these calculations are the same as those used for the estimation of the size of the domains assuming that D in the gel is only able to transfer to one of the fluid phases (the one that is considered to be surrounding the gel domains), whereas D in the fluid is able to transfer to both fluid phases. In addition, it is necessary to take into account the amount of gel phase, the partition of D into the gel phase, the surface density of A in each of the fluid phases and the size of the gel domains assuming that A are excluded from these domains (i.e., taking into account an exclusion distance). The lipid lateral organization predicted using the FRET formalisms, where l_o phase is surrounding Cer-enriched gel phase, is in good agreement with the one observed by AFM in similar systems [106–108].

Cer-effects on raft mixtures containing high Chol concentration are much less pronounced and that is reflected by a similar variation of FRET efficiency in the absence and presence of Cer, independently of the D/A pairs used for the study. The calculation of the expected FRET efficiency for *t*-PnA/*N*-NBD-18:1,18:1 PE D/A 3 pair assuming that Cer-gel domains are always formed undoubtedly confirms that Cer's ability to segregate into these domains decreases with Chol content, because an higher difference between the theoretical and the experimental FRET efficiencies is obtained (Fig. 5). For this model the size of the gel domains must be taken into account. In addition it is assumed that the same gel phase fraction (15% in this case) is formed for all the raft mixtures and D and A distribute randomly between the fluid phases. This latter assumption is valid for the *t*-PnA/*N*-NBD-18:1,18:1 PE D/A 3 pair because both probes partition equally between l_d and l_o phases. On the other hand, when this model is applied to *t*-PnA/*N*-NBD-16:0,16:0 PE D/A 2 pair it allows validating the existence of the two fluid phases because, if only one fluid phase were present then the theoretical and experimental FRET efficiencies should be equal (Fig. 5). In this case, the values are different showing that A are not randomly distributed in the fluid phase, and therefore fluid/fluid heterogeneity is present in the mixtures.

The FRET formalisms presented here, based on the combination of data obtained from multiple D/A pairs, were developed and applied to the study of a particular system: Cer-containing raft mixtures. However, this type of considerations can be applied to the study of other systems exhibiting phase separation, and the degree of complexity of the system under study will determine the number and type of D/A pairs that must be chosen. Therefore, to study the lipid

lateral organization of a certain lipid membrane the FRET pairs should be adequate to each of the phases present in the system and in particular to the type of lipid reorganization to be explored. In addition, the partition coefficient of the probes must be determined to the particular phases under study, because the physical properties of the phases change according to the lipids present (e.g. a Cer-gel phase is physically different from a SM-gel phase [64,76]). This is also valid for the photophysical parameters of the probes that need to be determined for a given phase. Only under these conditions is possible to obtain a whole set of information on amount and nature of the phases present, lipid lateral organization and size of the domains formed.

4.5. FRET studies of nano and microdomains of lipids and proteins in cell membranes

In cellular membranes, due to the high number of lipid and protein components, and their non-equilibrium state, the direct application of phase diagrams is precluded. Many limitations come also from the fact that most visible probes contain bulky fluorophores that are excluded from or strongly perturb Chol, sphingolipid-enriched domains, whereas UV-excited probes (*t*-PnA, DHE, filipin, nystatin, DPH) are more demanding in terms of optics and many of them are cytotoxic [109]. We give here some examples of how important information has been taken from FRET studies in relation to lipid domains and rafts in cells, either using or circumventing the aforementioned complexities.

A model has been presented that accounts for one of the most common experimental designs for FRET in cell membranes in lipid microdomains studies: the case where donor and acceptor label separately two probing proteins (usually antibodies, but also e.g., the raft marker CTB) [110]. In this situation, only one *trans* transfer is considered, because the two labeled proteins usually present the fluorophore in different planes and transfer to the opposite leaflet is negligible. The authors introduce the labeling ratio and the probing proteins are modeled as a sphere [110]. Because both D and A are labeling the same protein, the raft/non-raft K_p is the same for both. Additionally, the donor's decay (quantum yield, R_0 , etc.) is also phase independent because it is in a proteic environment. Assuming that rafts are randomly distributed and their area fraction is related to the protein expression level, the authors obtain simple integrated equations for FRET efficiency [110]. This model is then applied to the crude data from the paradigmatic paper by Kenworthy and Edidin [111], where clusters or domains had not been detected, though their presence in a small amount, i.e., incorporating up to 20% of the labeling protein, was not discarded. The application of the model by Acasandrei et al. [110] to the same data gave further quantitative support to the presence of lipid rafts.

Another example of a careful analysis of FRET data, combined with an elegant experimental approach highlighting the advantages of post-translational labeling methods in which the donor/acceptor ratios can be controlled very precisely is the work by Meyer et al. [112]. In this study of the lateral organization of the plasma membrane of a prototypical G-protein coupled receptor, their FRET data ruled out the formation of any kind of oligomer, and could only be explained by a model where the receptor resides in cholesterol-sensitive microdomains, with a local concentration ~80 times higher than the average concentration in the whole membrane, and that those domains have a size below optical resolution (~10 nm diameter) and occupy ~1% of the total membrane surface area.

The technique of fusion of inositolide-recognizing protein modules to fluorescent proteins has become one of the most popular tools to study PI dynamics in live cells. In the review by Várnai and Balla [113] they emphasize the controversial points and the guiding principles that should be taken into account when interpreting experimental data, including from FRET experiments. One interesting feature of this review is that the guidelines and principles can be generalized to the

use of fluorescently-labeled lipid-binding protein domains or to proteins fused to fluorescent proteins to the study of the behavior of lipids and lipid domains in cells.

Recently, a model was derived for a case where FRET (e.g., between CFP and YFP tagged proteins) may occur intramolecularly, intermolecularly, or both, and their relative dependence on the formation of aggregates— dimers, trimers, and higher order [114]. Both from the model and experiments in cells, the authors verify that in the case of intramolecular FRET the efficiency of the process is affected by the aggregation state only to a very small extent. In addition, comparing the results in fixed and live cells, it is concluded that the fixation process decreases significantly the FRET efficiency in the intramolecular case, probably by conformational restrictions affecting the κ^2 value (see Eq. 2) for the FRET pair.

A few studies in which the FRET efficiency is obtained from lifetime measurements under the microscope (fluorescence lifetime imaging microscopy, FLIM) have been made, namely the raft dependent interaction of tetanus neurotoxin with Thy-1 [115], and the interaction between BACE (β site of amyloid precursor protein-cleaving enzyme) and the low density lipoprotein receptor-related protein occurring on lipid rafts at the cell surface [116].

More recently, a FRET-FLIM study has been conducted in order to relate EGF receptor (EGFR) activation to the reorganization of different lipid microdomains [117]. For reliable interpretation of the FLIM results, the specific, non-agonistic and monovalent labeling of EGFR is a pre-requisite. To this purpose, the authors raised antibodies from *Llama glama* that are devoid of light chains [118], and made a library of the variable heavy chain region of those antibodies directed against EGFR. Whereas the common co-localization procedure applied to confocal fluorescence intensity images allowed observing co-localization at the micrometer level, and e.g. in this case both EGF and transferrin receptors co-localized with GM1 and GPI-CFP (both raft markers), the FRET-FLIM technique confirmed that, at the nanometer scale, GM1 co-localizes with EGFR, but not with the non-raft transferrin receptor [117].

In cells, one common simplification is to assume two types of domains e.g. raft/non-raft or ordered/disordered, and then the results can be compared to e.g. the *l*/*o* coexistence on a lipid phase diagram in a ternary model system. Due to intrinsic limitations such as cell stability, and because usually in cells microscopy studies are carried out (in order to control cell state, and to know the fluorophore localization, and use the signal coming only from the (sub)cellular membrane of interest) fluorescence intensity decays with a high number of photons (demanding e.g., longer acquisition times; [82]) with low background, etc., necessary to perform global analysis with equations like those presented in Section 3 are currently not feasible. Usually, steady-state data is obtained, and the integration of the model is thus required. Even when lifetime data is obtained (FRET-FLIM) the number of counts allows only obtaining the lifetime-weighted quantum yield and calculating the FRET efficiency from Eq. 3. However, from the examples given above, it is clear that the interpretation of observed FRET efficiencies can depend on considerable theoretical modelling and concomitant assumptions [109].

The experimental methods for visualizing membrane microdomains and quantifying FRET efficiencies in FRET microscopy with emphasis on novel strategies have been reviewed elsewhere [119–122]. Several approaches were developed in order to explore, on the nanoscale range, the specific interactions among proteins, lipids or lipids and proteins in live cells. Homo-FRET microscopy was successfully used to study, e.g., the clustering among GPI-anchored folate receptors within distinct lipid raft domains [83,123] and the oligomerization of hedgehog [124], while hetero- and homo-FRET were applied to the study of lipid lateral organization in cell membranes [86]. In the latter work, lipid probes were used, instead of the commonly employed fluorescent proteins, and nanoscale

heterogeneity could be detected at the lipid level, which was dependent on cholesterol content and membrane perturbations by external agents.

5. Concluding remarks

The examples described in the preceding section illustrate the utility and versatility of FRET-based methodologies in the study of heterogeneity and phase separation in membrane systems. In our 2001 review [22], we stated that “Given its unique features (namely, the strong dependence of the transfer rate on the distance and local concentration), it is surprising that the number of quantitative (especially time-resolved) studies of RET in detection and characterization of lipid distribution heterogeneity and phase separation are so few”. Less than one decade later, the situation has undoubtedly changed, as increasingly more researchers are aware of the power of FRET as a tool to study membrane nanoheterogeneity. Whereas the most quantitative applications such as direct analysis of decay kinetics rather than FRET integrated efficiency are obviously still found predominantly in the study of simpler one/two-phase model systems, formalisms with a reasonable amount of approximations and directed to the analysis of data obtain under the microscope are regularly emerging. These recent developments bode well for the continuation of increased success of FRET in the study of heterogeneity at all levels of membrane complexity.

Acknowledgements

Financial support for this work was provided by FCT (Portugal) through projects PPCDT/QUI/57123/2004 and PTDC/QUI/68151/2006. L.C.S. acknowledges grant BPD/30289/2006 from FCT (Portugal).

References

- [1] S.J. Singer, G.L. Nicholson, The fluid mosaic model of the structure of cell membranes, *Science* 175 (1972) 720–731.
- [2] D. Marsh, *Handbook of Lipid Bilayers*, CRC Press, Boca Raton, FL, 1990.
- [3] J.H. Ipsen, G. Karlstrom, O.G. Mouritsen, H. Wennerstrom, M.J. Zuckermann, Phase equilibria in the phosphatidylcholine–cholesterol system, *Biochim. Biophys. Acta* 905 (1987) 162–172.
- [4] K. Simons, E. Ikonen, Functional rafts in cell membranes, *Nature* 387 (1997) 569–572.
- [5] P.F.F. Almeida, W.L.C. Vaz, T.E. Thompson, Lateral diffusion and percolation in two-phase, two-component lipid bilayers. Topology of the solid-phase domains in-plane and across the lipid bilayer, *Biochemistry* 31 (1992) 7198–7210.
- [6] R.F.M. de Almeida, L.M.S. Loura, A. Fedorov, M. Prieto, Nonequilibrium phenomena in the phase separation of a two-component lipid bilayer, *Biophys. J.* 82 (2002) 823–834.
- [7] K. Jørgensen, A. Klinger, R.L. Biltonen, Nonequilibrium lipid domain growth in the gel–fluid two phase region of a DC16PC–DC22PC lipid mixture investigated by Monte-Carlo computer simulation, FT-IR and fluorescence spectroscopy, *J. Phys. Chem.* 104 (2000) 11763–11773.
- [8] K. Simons, W.L.C. Vaz, Model systems, lipid rafts, and cell membranes, *Annu. Rev. Biophys. Biomol. Struct.* 33 (2004) 269–295.
- [9] S. Mayor, M. Rao, Rafts: scale-dependent, active lipid organization at the cell surface, *Traffic* 5 (2004) 231–240.
- [10] K. Jacobson, O.G. Mouritsen, R.G. Anderson, Lipid rafts: at a crossroad between cell biology and physics, *Nat. Cell Biol.* 9 (2007) 7–14.
- [11] A. Kusumi, C. Nakada, K. Ritchie, K. Murase, K. Suzuki, H. Murakoshi, R.S. Kasai, J. Kondo, T. Fujiwara, Paradigm shift of the plasma membrane concept from the two-dimensional continuum fluid to the partitioned fluid: high-speed single-molecule tracking of membrane molecules, *Annu. Rev. Biophys. Biomol. Struct.* 34 (2005) 351–378.
- [12] S.L. Veatch, S.L. Keller, Separation of liquid phases in giant vesicles of ternary mixtures of phospholipids and cholesterol, *Biophys. J.* 85 (2003) 3074–3083.
- [13] S.L. Veatch, S.L. Keller, Miscibility phase diagrams of giant vesicles containing sphingomyelin, *Phys. Rev. Lett.* 94 (2005) 148101–148104.
- [14] C. Chachaty, D. Rainteau, C. Tessier, P.J. Quinn, C. Wolf, Building up of the liquid-ordered phase formed by sphingomyelin and cholesterol, *Biophys. J.* 88 (2005) 4032–4044.
- [15] P.F.F. Almeida, A. Pokorny, A. Hinderliter, Thermodynamics of membrane domains, *Biochim. Biophys. Acta* 1720 (2005) 1–13.
- [16] D. Evanko, STEDy progress, *Nat. Methods* 3 (2006) 661.
- [17] S. Chiantia, N. Kahya, P. Schwillie, Raft domain reorganization driven by short- and long chain ceramide: a combined AFM and FCS study, *Langmuir* 23 (2007) 7659–7665.
- [18] S. Karmakar, V.A. Raghunathan, S. Mayor, Phase behaviour of dipalmitoylphosphatidylcholine (DPPC)-cholesterol membranes, *J. Phys. Condens. Matter* 17 (2005) S1177–S1182.
- [19] S.L. Veatch, S.L. Keller, K. Gawrisch, Critical fluctuations in domain-forming lipid mixtures, *Proc. Natl. Acad. Sci. U. S. A.* 104 (2007) 17650–17655.
- [20] A.J. Garcia-Saez, S. Chiantia, P. Schwillie, Effect of line tension on the lateral organization of lipid membranes, *J. Biol. Chem.* 282 (2007) 33537–33544.
- [21] C.D. Blanchette, W.C. Lin, C.A. Orme, T.V. Ratto, M.L. Longo, Domain nucleation rates and interfacial line tensions in supported bilayers of ternary mixtures containing galactosylceramide, *Biophys. J.* 94 (2008) 2691–2697.
- [22] L.M.S. Loura, R.F.M. de Almeida, M. Prieto, Detection and characterization of membrane microheterogeneity by resonance energy transfer, *J. Fluoresc.* 11 (2001) 197–209.
- [23] L.M.S. Loura, R.F.M. de Almeida, M. Prieto, Methodologies and formalisms of resonance energy transfer in biophysics. Application to membrane model systems, *Int. J. Photoenergy* 5 (2003) 223–231.
- [24] T.H. Förster, Experimentelle und theoretische Untersuchung des Zwischenmolekularen Übergangs von Elektrizitätsenergie, *Z. Naturforsch.* 4a (1949) 321–327.
- [25] B. Van Der Meer, G. Coker III, S.-Y.S. Chen, *Resonance Energy Transfer: Theory and Data*, VCH Publishers, New York, 1994.
- [26] L. Stryer, Fluorescence energy transfer as a spectroscopic ruler, *Ann. Rev. Biochem.* 47 (1978) 829–846.
- [27] A.G. Tweet, W.D. Bellamy, G.L. Gaines Jr., Fluorescence quenching and energy transfer in monomolecular films containing chlorophyll, *J. Chem. Phys.* 41 (1964) 2068–2077.
- [28] P.K. Wolber, B.S. Hudson, An analytical solution to the Förster energy transfer problem in two dimensions, *Biophys. J.* 28 (1979) 197–210.
- [29] L. Davenport, R.E. Dale, R.H. Bisby, R.B. Cundall, Transverse location of the fluorescent probe 1,6-diphenyl-1,3,5-hexatriene in model lipid bilayer membrane systems by resonance energy transfer, *Biochemistry* 24 (1985) 4097–4108.
- [30] C.R. Mateo, R.F.M. de Almeida, L.M.S. Loura, M. Prieto, From lipid phases to membrane protein organization: fluorescence methodologies on the study of lipid–protein interaction, in: C.R. Mateo, J. Gómez, J. Villalain, J.M. González-Ros (Eds.), *Protein–Lipid Interactions*, Springer, New York, 2006, pp. 1–33.
- [31] L.M.S. Loura, A. Fedorov, M. Prieto, Partition of membrane probes in a gel/fluid two-component lipid system: a fluorescence resonance energy transfer study, *Biochim. Biophys. Acta* 1467 (2000) 101–112.
- [32] P. Ballet, M. Van der Auweraer, F.C. De Schryver, H. Lemmetyinen, E. Vuorimaa, Global analysis of the fluorescence decays of N,N'-diiododecyl rhodamine B in Langmuir–Blodgett films of diacylphosphatidic acids, *J. Phys. Chem.* 100 (1996) 13701–13715.
- [33] L.M.S. Loura, A. Fedorov, M. Prieto, Fluid–fluid membrane micro-heterogeneity: a fluorescence resonance energy transfer study, *Biophys. J.* 80 (2001) 776–788.
- [34] K.B. Towles, N. Dan, Determination of membrane domain size by fluorescence resonance energy transfer: effects of domain polydispersity and packing, *Langmuir* 23 (2007) 4737–4739.
- [35] J.T. Buboltz, Steady-state probe-partitioning FRET: A simple and robust tool for the study of membrane phase behavior, *Phys. Rev. E* 76 (2007) 021903.
- [36] J.T. Buboltz, C. Bwalya, S. Reyes, D. Kamburov, Stern–Volmer modeling of steady-state Förster energy transfer between dilute, freely diffusing membrane-bound fluorophores, *J. Chem. Phys.* 127 (2007) 215101.
- [37] K.B. Towles, A.C. Brown, S.P. Wrenn, N. Dan, Effect of membrane microheterogeneity and domain size on fluorescence resonance energy transfer, *Biophys. J.* 93 (2007) 655–667.
- [38] Y.S. Liu, L. Li, S. Ni, M. Winnik, Recovery of acceptor concentration distribution in direct energy transfer experiments, *Chem. Phys.* 177 (1993) 579–589.
- [39] L.M.S. Loura, A. Fedorov, M. Prieto, Membrane probe distribution heterogeneity: a resonance energy transfer study, *J. Phys. Chem. B* 104 (2000) 6920–6931.
- [40] A.C. Brown, K.B. Towles, S.P. Wrenn, Measuring raft size as a function of membrane composition in PC-based systems: part I- binary systems, *Langmuir* 23 (2007) 11180–11187.
- [41] L. Bagatolli, E. Gratton, Two photon fluorescence microscopy of coexisting lipid domains in giant unilamellar vesicles of binary phospholipid mixtures, *Biophys. J.* 78 (2000) 290–305.
- [42] B.K. Fung, L. Stryer, Surface density determination in membranes by fluorescence energy transfer, *Biochemistry* 17 (1978) 5241–5248.
- [43] C. Gutiérrez-Merino, Quantitation of the Förster energy transfer for two-dimensional systems. I. Lateral phase separation in unilamellar vesicles formed by binary phospholipid mixtures, *Biophys. Chem.* 14 (1981) 247–257.
- [44] C. Gutiérrez-Merino, Quantitation of the Förster energy transfer for two-dimensional systems. II. Protein distribution and aggregation state in biological membranes, *Biophys. Chem.* 14 (1981) 259–266.
- [45] J. Silvius, Fluorescence energy transfer reveals microdomain formation at physiological temperatures in lipid mixtures modeling the outer leaflet of the plasma membrane, *Biophys. J.* 85 (2003) 1034–1045.
- [46] B. Snyder, E. Freire, Fluorescence energy transfer in two dimensions. A numeric solution for random and non-random distributions, *Biophys. J.* 40 (1982) 137–148.
- [47] L.M.S. Loura, M. Prieto, Resonance energy transfer in heterogeneous planar and bilayer systems: theory and simulation, *J. Phys. Chem. B* 104 (2000) 6911–6919.
- [48] C. Gutiérrez-Merino, F. Munkonge, A.M. Mata, J.M. East, B.L. Levinson, R.M. Napier, A.G. Lee, The position of the ATP binding site on the (Ca²⁺+Mg²⁺)-ATPase, *Biochim. Biophys. Acta* 897 (1987) 207–216.

- [49] F.M. Fernandes, L.M.S. Loura, R. Koehorst, R.B. Spruijt, M.A. Hemminga, M. Prieto, Quantification of protein–lipid selectivity using FRET. Application to the M13 major coat protein, *Biophys. J.* 87 (2004) 344–352.
- [50] R.C. Capeta, J.A. Poveda, L.M.S. Loura, Non-uniform membrane probe distribution in resonance energy transfer: application to protein–lipid selectivity, *J. Fluoresc.* 16 (2006) 161–172.
- [51] L.M.S. Loura, A. Fedorov, M. Prieto, Resonance energy transfer in a model system of membranes: application to gel and liquid crystalline phases, *Biophys. J.* 71 (1996) 1823–1836.
- [52] D.A. Redfern, A. Gericke, pH-dependent domain formation in phosphatidylinositol polyphosphate/phosphatidylcholine mixed vesicles, *J. Lipid Res.* 46 (2005) 504–515.
- [53] F. Fernandes, L.M.S. Loura, A. Fedorov, M. Prieto, Absence of clustering of phosphatidylinositol-(4,5)-bisphosphate in fluid phosphatidylcholine, *J. Lipid Res.* 47 (2006) 1521–1525.
- [54] A. Holt, R.F.M. de Almeida, T.K. Nyholm, L.M.S. Loura, A.E. Daily, R.W. Staffhorst, D.T. Rijkers, R.E. Koeppe II, M. Prieto, J.A. Killian, Is there a preferential interaction between cholesterol and tryptophan residues in membrane proteins? *Biochemistry* 47 (2008) 2638–2649.
- [55] R.F.M. de Almeida, L.M.S. Loura, M. Prieto, A. Watts, A. Fedorov, F.J. Barrantes, Cholesterol modulates the organization of the γ M4 transmembrane domain of the muscle nicotinic acetylcholine receptor, *Biophys. J.* 86 (2004) 2261–2272.
- [56] S. Degroote, J. Wolthoorn, G. Van Meer, The cell biology of glycosphingolipids, *Semin. Cell Dev. Biol.* 15 (2004) 375–387.
- [57] S. Mabrey, J.M. Sturtevant, Investigation of phase transitions of lipids and lipid mixtures by high sensitivity differential scanning calorimetry, *Proc. Natl. Acad. Sci.* 73 (1976) 3862–3866.
- [58] O.G. Mouritsen, K. Jørgensen, Dynamical order and disorder in lipid bilayers, *Chem. Phys. Lipids* 73 (1994) 3–25.
- [59] C. Bezombes, S. Grazide, C. Garret, C. Fabre, A. Quillet-Mary, S. Müller, J.-P. Jaffrézou, G. Laurent, Rituximab antiproliferative effect in B-lymphoma cells is associated with acid-sphingomyelinase activation in raft microdomains, *Blood* 104 (2004) 1166–1173.
- [60] S. Mathias, L.A. Peña, R.N. Kolesnick, Signal transduction of stress via ceramide, *Biochem. J.* 335 (1998) 465–480.
- [61] P.P. Ruvolo, Intracellular signal transduction pathways activated by ceramide and its metabolites, *Pharmacol. Res.* 47 (2003) 383–392.
- [62] R.N. Kolesnick, F.M. Göni, A. Alonso, Compartmentalization of ceramide signaling: physical foundation and biological effects, *J. Cell. Physiol.* 184 (2000) 285–300.
- [63] A.E. Cremesti, F.M. Göni, R.N. Kolesnick, Role of sphingomyelinase and ceramide in modulating rafts: do biophysical properties determine biological outcome? *FEBS Lett.* 531 (2002) 47–53.
- [64] L. Silva, R.F.M. de Almeida, A.P. Matos, A. Fedorov, M. Prieto, Ceramide-platform formation and-induced biophysical changes in a fluid phospholipid membrane, *Mol. Membr. Biol.* 23 (2006) 137–150.
- [65] C.R. Mateo, J.-C. Brochon, M.P. Lillo, A.U. Acuña, Lipid clustering in bilayers detected by the fluorescence kinetics and anisotropy of trans-parinaric acid, *Biophys. J.* 65 (1993) 2237–2247.
- [66] B. Lentz, Membrane “fluidity” from fluorescence anisotropy measurements, in: L. Loew (Ed.), *Spectroscopic Membrane Probes: Volume I*, CRC, Boca Raton, FL, 1988, pp. 13–41.
- [67] L. Davenport, Fluorescence probes for studying membrane heterogeneity, *Meth. Enzymol.* 278 (1997) 487–512.
- [68] W.L.C. Vaz, E. Melo, Fluorescence spectroscopic studies on phase heterogeneity in lipid bilayer membranes, *J. Fluoresc.* 11 (2002) 255–271.
- [69] M.R. Vist, J.H. Davis, Phase equilibria of cholesterol/dipalmitoylphosphatidylcholine mixtures: 2 H nuclear magnetic resonance and differential scanning calorimetry, *Biochemistry* 29 (1990) 451–464.
- [70] M.B. Sankaram, T.E. Thompson, Cholesterol-induced fluid-phase immiscibility in membranes, *Proc. Natl. Acad. Sci. U. S. A.* 88 (1991) 8686–8690.
- [71] M.J.L. de Lange, M. Bonn, M. Müller, Direct measurement of phase coexistence in DPPC/cholesterol vesicles using Raman spectroscopy, *Chem. Phys. Lipids* 146 (2007) 76–84.
- [72] Y.-W. Chiang, A.J. Costa-Filho, J.H. Freed, Dynamic molecular structure and phase diagram of DPPC–cholesterol binary mixtures: a 2D-ELDOR study, *J. Phys. Chem. B* 111 (2007) 11260–11270.
- [73] P.F.F. Almeida, W.L.C. Vaz, T.E. Thompson, Lateral diffusion in the liquid-phases of dimyristoylphosphatidylcholine/cholesterol lipid bilayers— a free-volume analysis, *Biochemistry* 31 (1992) 6739–6747.
- [74] C.R. Mateo, A.U. Acuña, J.-C. Brochon, Liquid-crystalline phases of cholesterol lipid bilayers as revealed by the fluorescence of trans-parinaric acid, *Biophys. J.* 68 (1995) 978–987.
- [75] J.L. Thewalt, M. Bloom, Phosphatidylcholine-cholesterol phase-diagrams, *Biophys. J.* 63 (1992) 1176–1181.
- [76] R.F.M. de Almeida, A. Fedorov, M. Prieto, Sphingomyelin/Phosphatidylcholine/Cholesterol phase diagram: boundaries and composition of lipid rafts, *Biophys. J.* 85 (2003) 2406–2416.
- [77] L. Silva, A. Coutinho, A. Fedorov, M. Prieto, Competitive binding of cholesterol and ergosterol to the polyene antibiotic nystatin. A fluorescence study, *Biophys. J.* 90 (2006) 3625–3631.
- [78] Y.-W. Hsueh, M.-T. Chen, P.J. Patty, C. Code, J. Cheng, B.J. Frisken, M. Zuckermann, J. Thewalt, Ergosterol in POPC membranes: physical properties and comparison with structurally similar sterols, *Biophys. J.* 92 (2007) 1606–1615.
- [79] M.B. Sankaram, T.E. Thompson, Interaction of cholesterol with various glycerophospholipids and sphingomyelin, *Biochemistry* 29 (1990) 10670–10675.
- [80] M.I. Collado, F.M. Göni, A. Alonso, D. Marsh, Domain formation in sphingomyelin/cholesterol mixed membranes studied by spin-label electron spin resonance spectroscopy, *Biochemistry* 44 (2005) 4911–4918.
- [81] Z. Arsov, L. Quaroni, Detection of lipid phase coexistence and lipid interactions in sphingomyelin/cholesterol membranes by ATR-FTIR spectroscopy, *Biochim. Biophys. Acta* 1778 (2008) 880–889.
- [82] R.F.M. de Almeida, J. Borst, A. Fedorov, M. Prieto, A.J.W.G. Visser, Complexity of lipid domains and rafts in giant unilamellar vesicles revealed by combining imaging and microscopic and macroscopic time-resolved fluorescence, *Biophys. J.* 93 (2007) 539–553.
- [83] R. Varma, S. Mayor, GPI-anchored proteins are organized in submicron domains at the cell surface, *Nature* 394 (1998) 798–801.
- [84] I.A. Prior, C. Muncke, R.G. Parton, J.F. Hancock, Direct visualization of Ras proteins in spatially distinct cell surface microdomains, *J. Cell Biol.* 160 (2003) 165–170.
- [85] D.V. Nicolau Jr., K. Burrage, R.G. Parton, J.F. Hancock, Identifying optimal lipid raft characteristics required to promote nanoscale protein–protein interactions on the plasma membrane, *Mol. Cell. Biol.* 26 (2006) 313–323.
- [86] P. Sengupta, D. Holowka, B. Baird, Fluorescence resonance energy transfer between lipid probes detects nanoscopic heterogeneity in the plasma membrane of live cells, *Biophys. J.* 92 (2007) 3564–3574.
- [87] C. Dietrich, L.A. Bagatolli, Z.N. Volovyk, N.L. Thompson, M. Levi, K. Jacobson, E. Gratton, Lipid rafts reconstituted in model membranes, *Biophys. J.* 80 (2001) 1417–1428.
- [88] R.F.M. de Almeida, L.M.S. Loura, A. Fedorov, M. Prieto, Lipid rafts have different sizes depending on membrane composition: a time-resolved fluorescence resonance energy transfer study, *J. Mol. Biol.* 346 (2005) 1109–1120.
- [89] L.C. Silva, R.F.M. de Almeida, B.M. Castro, A. Fedorov, M. Prieto, Ceramide-domain formation and collapse in lipid rafts: membrane reorganization by an apoptotic lipid, *Biophys. J.* 92 (2007) 502–516.
- [90] M.L. Frazier, J.R. Wright, A. Pokorny, P.F.F. Almeida, Investigation of domain formation in sphingomyelin/cholesterol/POPC mixtures by fluorescence resonance energy transfer and Monte Carlo simulations, *Biophys. J.* 92 (2007) 2422–2433.
- [91] A. Pokorny, L.E. Yandek, A.I. Elegbede, A. Hinderliter, P.F.F. Almeida, Temperature and composition dependence of the interaction of D-lysine with ternary mixtures of sphingomyelin/cholesterol/POPC, *Biophys. J.* 91 (2006) 2184–2197.
- [92] J.T. Buboltz, C. Bwalya, K. Williams, M. Schutzer, High-resolution mapping of phase behavior in a ternary lipid mixture: do lipid-raft phase boundaries depend on the sample preparation procedure? *Langmuir* 23 (2007) 11968–11971.
- [93] S.L. Veatch, I.V. Polozov, K. Gawrisch, S.L. Keller, Liquid domains in vesicles investigated by NMR and fluorescence microscopy, *Biophys. J.* 86 (2004) 2910–2922.
- [94] A.C. Brown, K.B. Towles, S.P. Wrenn, Measuring raft size as a function of membrane composition in PC-based systems: part II- ternary systems, *Langmuir* 23 (2007) 11188–11196.
- [95] S.A. Pandit, S.-W. Chiu, E. Jakobsson, A. Grama, H.L. Scott, Cholesterol packing around lipids with saturated and unsaturated chains: a simulation study, *Langmuir* 24 (2008) 6858–6865.
- [96] F. Fernandes, L.M.S. Loura, M. Prieto, R. Koehorst, R. Spruijt, M.A. Hemminga, Dependence of M13 major coat protein oligomerization and lateral segregation on bilayer composition, *Biophys. J.* 85 (2003) 2430–2441.
- [97] S.N. Pinto, L.C. Silva, R.F.M. de Almeida, M. Prieto, Membrane domain formation, interdigitation and morphological alterations induced by the very long chain asymmetric C24:1 ceramide, *Biophys. J.* 95 (2008) 2867–2879.
- [98] Y.W. Hsueh, R. Giles, N. Kitson, J. Thewalt, The effect of ceramide on phosphatidylcholine membranes: a deuterium NMR study, *Biophys. J.* 82 (2002) 3089–3095.
- [99] J.M. Holopainen, J. Lemmich, F. Richter, O.G. Mouritsen, G. Rapp, P.K.J. Kinnunen, Dimyristoylphosphatidylcholine/C16:0-ceramide binary liposomes studied by differential scanning calorimetry and wide- and small-angle X-ray scattering, *Biophys. J.* 78 (2000) 2459–2469.
- [100] J.M. Holopainen, H.L. Brockman, R.E. Brown, P.K.J. Kinnunen, Interfacial interactions of ceramide with dimyristoylphosphatidylcholine: impact of the N-acyl chain, *Biophys. J.* 80 (2001) 765–775.
- [101] D.C. Carrer, S. Schreier, M. Patrino, B. Maggio, Effects of a short-chain ceramide on bilayer domain formation, thickness, and chain mobility: DMPC and asymmetric ceramide mixtures, *Biophys. J.* 90 (2006) 2394–2403.
- [102] D.C. Carrer, B. Maggio, Phase behavior and molecular interactions in mixtures of ceramide with dipalmitoylphosphatidylcholine, *J. Lipid Res.* 40 (1999) 1978–1989.
- [103] J. Sot, L.A. Bagatolli, F.M. Göni, A. Alonso, Detergent-resistant, ceramide-enriched domains in sphingomyelin/ceramide bilayers, *Biophys. J.* 90 (2006) 903–914.
- [104] B.M. Castro, R.F.M. de Almeida, L.C. Silva, A. Fedorov, M. Prieto, Formation of Ceramide/Sphingomyelin gel domains in the presence of an unsaturated phospholipid: a quantitative multiprobe approach, *Biophys. J.* 93 (2007) 1639–1650.
- [105] C.R. Bollinger, V. Teichgraber, E. Gulbins, Ceramide-enriched membrane domains, *Biochim. Biophys. Acta* 1746 (2005) 284–294.
- [106] I. Johnston, L.J. Johnston, Ceramide promotes restructuring of model raft membranes, *Langmuir* 22 (2006) 11284–11289.
- [107] I. Johnston, L.J. Johnston, Sphingomyelinase generation of ceramide promotes clustering of nanoscale domains in supported bilayer membranes, *Biochim. Biophys. Acta* 1778 (2008) 185–197.
- [108] S. Chiantia, N. Kahya, J. Ries, P. Schwille, Effects of ceramide on liquid-ordered domains investigated by simultaneous AFM and FCS, *Biophys. J.* 90 (2006) 4500–4508.

- [109] B.C. Lagerholm, G.E. Weinreb, K. Jacobson, N.L. Thompson, Detecting microdomains in intact cell membranes, *Annu. Rev. Phys. Chem.* 56 (2005) 309–336.
- [110] M.A. Acasandrei, R.E. Dale, M. VandeVen, M. Ameloot, Two-dimensional Förster resonance energy transfer (2-D FRET) and the membrane raft hypothesis, *Chem. Phys. Lett.* 419 (2006) 469–473.
- [111] A.K. Kenworthy, M. Edidin, Distribution of a glycosylphosphatidylinositol-anchored protein at the apical surface of MDCK cells examined at a resolution of <100 Å using imaging fluorescence resonance energy transfer, *J. Cell Biol.* 142 (1998) 69–84.
- [112] B.H. Meyer, J.-M. Segura, K.L. Martinez, R. Hovius, N. George, K. Johnsson, H. Vogel, FRET imaging reveals that functional neurokinin-1 receptors are monomeric and reside in membrane microdomains of live cells, *Proc. Natl. Acad. Sci. U. S. A.* 103 (2006) 2138–2143.
- [113] P. Várnai, T. Balla, Live cell imaging of phosphoinositide dynamics with fluorescent protein domains, *Biochim. Biophys. Acta* 1761 (2006) 957–967.
- [114] M. Anikovskiy, L. Dale, S. Ferguson, N. Petersen, Resonance energy transfer in cells: a new look at fixation effect and receptor aggregation on cell membrane, *Biophys. J.* 95 (2008) 1349–1359.
- [115] J. Herreros, T. Ng, G. Schiavo, Lipid rafts act as specialized domains for tetanus toxin binding and internalization into neurons, *Mol. Biol. Cell* 12 (2001) 2947–2960.
- [116] C.A.F. Von Arnim, A. Kinoshita, I.D. Peltan, M.M. Tangredi, L. Herl, B.M. Lee, R. Spoelgen, T.T. Hsieh, S. Ranganathan, F.D. Battey, C.X. Liu, B.J. Backsai, S. Sever, M.C. Irizarry, D.K. Strickland, B.T. Hyman, The low density lipoprotein receptor-related protein (LRP) is a novel beta-secretase (BACE1) substrate, *J. Biol. Chem.* 280 (2005) 17777–17785.
- [117] E.G. Hofman, M.O. Ruonala, A.N. Bader, D. van den Heuvel, J. Voortman, R.C. Roovers, A.J. Verkleij, H.C. Gerritsen, P.M.P. van Bergen en Henegouwen, EGF induces coalescence of different lipid rafts, *J. Cell Sci.* 121 (2008) 2519–2528.
- [118] K.E. Conrath, U. Wernery, S. Muyldermans, V.K. Nguyen, Emergence and evolution of functional heavy-chain antibodies in Camelidae, *Dev. Comp. Immunol.* 27 (2003) 87–103.
- [119] D.M. Owen, M.A.A. Neil, P.M.W. French, A.I. Magee, Optical techniques for imaging membrane lipid microdomains in living cells, *Sem. Cell Develop. Biol.* 18 (2007) 591–598.
- [120] E.A. Jares-Erijman, T.M. Jovin, Imaging molecular interactions in living cells by FRET microscopy, *Curr. Opin. Chem. Biol.* 10 (2006) 409–416.
- [121] M. Rao, S. Mayor, Use of Förster's resonance energy transfer microscopy to study lipid rafts, *Biochim. Biophys. Acta* 1746 (2005) 221–233.
- [122] S. Padilla-Parra, N. Auduge, M. Coppey-Moisan, M. Tramier, Quantitative FRET analysis by fast acquisition time domain FLIM at high spatial resolution in living cells, *Biophys. J.* 95 (2008) 2976–2988.
- [123] P. Sharma, R. Varma, R.C. Sarasij, Ira, K. Gousset, G. Krishnamoorthy, M. Rao, S. Mayor, Nanoscale organization of multiple GPI-anchored proteins in living cell membranes, *Cell* 116 (2004) 577–589.
- [124] N. Vyas, D. Goswami, A. Manonmani, P. Sharma, H.A. Ranganath, K. VijayRaghavan, L.S. Shashidhara, R. Sowdhamini, S. Mayor, Nanoscale organization of hedgehog is essential for long-range signalling, *Cell* 133 (2008) 1214–1227.